Glucagon-receptor signaling regulates energy metabolism via hepatic Farnesoid X Receptor and Fibroblast Growth Factor 21

[1]Teayoun Kim, [1]Shelly Nason, [1]Cassie Holleman, [2]Mark Pepin, [5]Landon Wilson, [5]Taylor F Berryhill, [2]Adam R. Wende, [3]Chad Steele, [4]Martin E. Young, [5]Stephen Barnes [6]Daniel J. Drucker, [7]Brian Finan, [7,8]Richard DiMarchi, [9]Diego Perez-Tilve, [10]Matthias Tschoep & [1]Kirk M Habegger[#]

[1]Comprehensive Diabetes Center and Department of Medicine - Endocrinology, Diabetes & and Metabolism, University of Alabama at Birmingham, Birmingham, AL USA
[2]Department of Pathology – Molecular & Cellular Pathology, University of Alabama at Birmingham, AL, USA
[3]Department of Medicine-Pulmonary/Allergy/Critical Care, University of Alabama at Birmingham, Birmingham, AL, USA
[4]Department of Medicine-Cardiovascular Disease, University of Alabama at Birmingham, Birmingham, AL, USA
[5]Department of Pharmacology, University of Alabama at Birmingham, Birmingham, AL, USA
[6]Lunenfeld-Tanenbaum Research Institute, Mt. Sinai Hospital, Department of Medicine, University of Toronto, Toronto, ON, CA
[7]Novo Nordisk Research Center Indianapolis, Indianapolis, IN, USA
[8]Dept. of Chemistry, Indiana University, Bloomington, IN, USA
[9]Metabolic Disease Institute, Div. of Endocrinology, Diabetes and Metabolism, University of Cincinnati, Cincinnati OH, USA
[10]Institute for Diabetes and Obesity, Helmholtz Zentrum München, München, Germany

[#] Correspondence to:
Kirk M Habegger
Dept. of Medicine - Endocrinology, Diabetes & Metabolism
University of Alabama at Birmingham
Birmingham, AL 35294
Email - kirkhabegger@uabmc.edu

The project described was supported by Award Number P30DK079626 from the National Institute of Diabetes and Digestive and Kidney Diseases, the American Diabetes Association grant 1-13-JF-21 (KMH), CIHR Grants 136942 and 154321 (DJD) as well as NIH grants K01 DK098319 and R01 DK112934 (KMH), and R01 DK077975 (DPT).

Key words:
Glucagon

FXR
FGF21
Obesity
Liver
Bile acid

Abstract

Glucagon, an essential regulator of glucose and lipid metabolism, also promotes weight loss, in part through potentiation of fibroblast-growth factor 21 (FGF21) secretion. However, FGF21 is only a partial mediator of metabolic actions ensuing from GcgR-activation, prompting us to search for additional pathways. Intriguingly, chronic GcgR agonism increases plasma bile acid levels. We hypothesized that GcgR agonism regulates energy metabolism, at least in part, through farnesoid X receptor (FXR). To test this hypothesis, we studied whole body and liver-specific FXR knockout ($Fxr^{\Delta liver}$) mice. Chronic GcgR agonist (IUB288) administration in diet-induced obese (DIO) *Gcgr*, *Fgf21* and *Fxr* whole body or liver-specific knockout ($^{\Delta liver}$) mice failed to reduce body weight (BW) when compared to wildtype (WT) mice. IUB288 increased energy expenditure and respiration in DIO WT mice, but not $FXR^{\Delta liver}$ mice. GcgR agonism increased [^{14}C]-palmitate oxidation in hepatocytes isolated from WT mice in a dose-dependent manner, an effect blunted in hepatocytes from $Fxr^{\Delta liver}$ mice. Our data clearly demonstrate that control of whole body energy expenditure by GcgR agonism requires intact FXR signaling in the liver. This heretofore-unappreciated aspect of glucagon biology has implications for the use of GcgR agonism in the therapy of metabolic disorders.

Introduction

Glucagon is secreted from pancreatic α-cells in response to hypoglycemia and is the primary counterregulatory hormone to insulin action, increasing glycogenolysis and gluconeogenesis, while simultaneously inhibiting glycogen synthesis(1). These actions, while beneficial in the context of hypoglycemia, may contribute to pathophysiological hyperglycemia in the setting of diabetes (2). GcgR agonism also modulates bile acid metabolism, stimulates fatty acid utilization, and reduces dyslipidemia, characteristics clearly desirable in anti-obesity therapeutics(1). It is now accepted that GcgR agonism, when coupled with glucagon-like peptide-1 (GLP-1) agonism, offers potential opportunities for the therapy of metabolic syndrome (3; 4).

We have reported that FGF21, secreted in response to GcgR agonism, mediates many glucagon actions, including the prevention of diet-induced obesity (5). Like glucagon, FGF21 regulates cholesterol and bile acid (BA) metabolism (6; 7). Similarly, the BA nuclear receptor FXR is a regulator of energy metabolism, mitochondrial function, and FGF21 gene expression (8). In this study, we investigated the roles of hepatic GCGR, FGF21, and FXR in the anti-obesity effects of the GcgR agonist IUB288.

Materials & Methods

Animal models. All studies were approved by and performed according to the guidelines of the Institutional Animal Care and Use Committee of the University of Alabama at Birmingham or the University of Cincinnati. Mice were single or group-housed on a 12:12-h light-dark cycle at 22°C and constant humidity with free access to food and water, except as noted. *Gcgr*- and *Fxr*-floxed mice were obtained from the original investigators (9; 10) while *Fgf21*- floxed and *Albumin*-Cre mice obtained from Jackson Labs (Bar Harbor, ME). All models were validated for tissue-specific, target gene knockout (Figure S1a-e). All mice maintained in our facilities are on a C57Bl/6J background. Mice were fed a standard chow (Teklad LM-485, 5.8% fat) for colony maintenance and high fat diet (HFD, 58.0 kcal% fat; D12331 Research Diets, New Brunswick NJ) for diet-induced obesity studies. For sacrifice, isoflurane anesthesia was used and torso blood was collected and plasma was collected by centrifugation of whole blood at 3,000 xg 10 minutes.

Peptides. IUB288 was synthesized as previously described (5) and native glucagon obtained from American Peptide Co.

Body composition and Indirect calorimetry. Body weight and food intake measurements were collected twice a week. Body composition was measured using magnetic resonance spectroscopy (EchoMRI, Echo Medical Systems). Combined indirect calorimetry was conducted as previously described (Comprehensive Laboratory Animal Monitoring System; Columbus Instruments)(11).

Glucose tolerance test. Intraperitoneal (IP) glucose (1.5 g/kg, 20% wt/vol d-glucose in 0.9% wt/vol saline, Sigma-Aldrich Corp., St. Louis, MO) tolerance tests were conducted in 5 h fasted mice as previously published (12). Tail vein blood glucose was assessed using a glucometer (TheraSense Freestyle glucometer, Abbott Laboratories, Abbott Park, IL).

Plasma & tissue analyses. Lipids in plasma and tissue samples from 2hr fasted mice were determined using Infinity™ Triglycerides (Thermo Scientific #TR22421), Infinity™ Cholesterol (Thermo Scientific #TR13421), Total Bile Acids Assay Kit (Crystal Chem. #80259), and β-Hydroxybutyrate (Ketone Body) Colorimetric Assay Kit (Cayman Chemicals. #700190). Bile acid profiling: Plasma aliquots (50 μl) were extracted to recover bile acids (see Supplemental Methods). Diluted extracts (1.25 μl plasma equivalent) were resolved by reverse-phase gradient liquid chromatography and analyzed by negative electrospray ionization mass spectrometry using multiple reaction monitoring. Bile acids peak areas were analyzed by MultiQuant™ 3.0.1 (SCIEX) and compared to peak-area-concentration standard curves of individual bile acids. Plasma hormones from 2 h fasted mice were determined by Bio-Plex Pro Mouse Diabetes 8-Plex Assay (Bio-Rad Laboratories) in plasma samples collected in the presence of protease and phosphatase Inhibitors (Halt, ThermoFisher).

Quantitative real-time PCR and RNA-Sequence analysis. Liver RNA was isolated from 2h fasted mice using the RNeasy Lipid Mini-Kit (Qiagen, Valencia, CA) and cDNA was synthesized by reverse transcription PCR using SuperScriptIII, DNase treatment, and anti-RNase treatment according to the manufacturer's instructions (Invitrogen, Carlsbad, CA). Single gene qPCR was performed as previously described (11). Data

were normalized to housekeeping genes *Hprt, Rps18,* or *Ppia* using the ΔΔct calculation. See Supplemental Table 1 for list of primer sets. High-throughput RNA sequencing was performed in the Heflin Genomics Core at the UAB. Gene network associations and differentially expressed genes (DEGs) identified via unpaired two-tailed and Bonferroni-adjusted P values (Q value) < 0.05, respectively. Sequencing data have been deposited within the Gene Expression Omnibus repository (https://www.ncbi.nlm.nih.gov/geo). Gene set enrichment analysis (GSEA), functional and network analyses, and candidate upstream regulators identified via QIAGEN's Ingenuity Pathway Analysis (IPA®, QIAGEN Redwood City, www.qiagen/ingenuity) where Fold-Change>1.5, P < 0.05, FPKM > 2.

Primary Hepatocyte Isolation. Primary hepatocytes were prepared from anesthetized mice as previously described(13). Perfusion (Krebs Ringer with glucose and 0.1 mM EGTA) followed by digestion buffer (Krebs Ringer with glucose, 1.4 mM $CaCl_2$, 50 µg/mL liberase [Roche, 05401119001]) was infused into the vena cava via peristaltic pump. Viable hepatocytes were recovered by Percoll gradient centrifugation (350xg 5 min) followed by washing (50xg 3 min, 3 times) and seeded on rat tail type 1 collagen-coated plates in DMEM (10% FBS, 1% Penicillin/Streptomycin) with all experiments conducted <24h post-isolation.

Statistics. All data are represented as mean and SEM. Statistical significance was determined using unpaired Student's *t*-tests or, where appropriate, one- and two-way analysis of variance (ANOVA) with multiple comparisons Tukey and Sidak post-test, respectively. Statistics were completed using GraphPad Prism version 7.0 for Macintosh

and Windows (GraphPad Software, San Diego, CA). Statistical significance was assigned when $P < 0.05$.

Results

Glucagon Promotes Body and Fat Mass Loss via Hepatic GcgRs.

We have previously reported that GcgR agonism reduces body and fat mass in diet-induced obese (DIO) mice (5). Considering the high level of GcgR expression in liver tissue, we reasoned that the anti-obesity signal may be hepatic in origin and tested this hypothesis utilizing mice deficient for hepatic *Gcgr* (*Gcgr*$^{\Delta liver}$) (9). 6-8 week old male, *Gcgr*$^{\Delta liver}$ mice and their littermate controls were placed on high-fat diet for 10 w to induce obesity. High fat feeding stimulated similar food intake and accumulation of body weight in both genotypes (Figure 1a-b). *Gcgr*$^{\Delta liver}$ mice exhibited slightly less fat mass and a trend for more lean mass (Figure 1c), with profoundly enhanced glucose tolerance as compared to their high-fat fed littermate controls (Figure 1d). Following high fat feeding, mice were matched for body weight and fat mass within each genotype and treated for 17d with vehicle (saline) or IUB288 (10 nmol/kg/day). *Gcgr*$^{\Delta liver}$ mice were protected from hyperglycemia following GcgR-agonism (Figure 2a). Chronic GcgR agonism significantly reduced body weight (Figures 2b and S1f) in WT mice, an effect mainly driven by fat mass loss with a modest decrease in lean mass (Figure 2c). In contrast, BW, fat, and lean mass, were preserved in IUB288-treated *Gcgr*$^{\Delta liver}$ mice (Figure 2b-c). IUB288 treatment reduced food intake in both genotypes, yet food consumption was not different between *Gcgr*$^{\Delta liver}$ mice and their littermate controls (Figure 2d).

We next examined the impact of GcgR agonism on circulating lipids. Chronic GcgR agonism significantly reduced circulating cholesterol (CHL) in WT, but not in *Gcgr*$^{\Delta liver}$ mice, with no effect on circulating TG (Figure 2e). Conversely, chronic GcgR agonism

significantly reduced hepatic TG levels in WT but not *Gcgr*$^{\Delta liver}$ mice, while liver CHL were unaffected by either genotype or treatment (Figure 2f). Altogether, these data demonstrate the regulatory role of hepatic GcgR in whole body energy balance, glucose, and lipid metabolism.

FGF21 and GcgR-stimulated Obesity Reversal.

We and others have reported that glucagon stimulates FGF21 secretion in hepatocytes(5; 14). To address the role of FGF21, obesity was induced via 16 weeks of high-fat feeding in 20 week old male, liver specific-*Fgf21* deficient (*Fgf21*$^{\Delta liver}$) and WT mice. Mice from each genotype were matched for body weight and fat mass and treated for 16d with vehicle (saline) or IUB288 (10 nmol/kg/day). Chronic GcgR agonism reduced BW (Figures 3a and S1g), food intake, fat, and lean mass in WT mice (Figure 3b-c). However, BW reduction in *Fgf21*$^{\Delta liver}$ mice was significantly blunted and GcgR-stimulated effects on body composition and food intake did not reach statistical significance (Figure 3a-c). Consistent with our prior findings(5), these data suggest that FGF21-dependent and -independent mechanisms mediate body and fat mass loss following GcgR agonism.

FXR Mediates GcgR-induced Body Weight Loss.

Glucagon regulates bile acid metabolism (1) and bile acids are known metabolic modulators (15). We sought to determine the contribution of bile acid metabolism in the effect of glucagon on BW. Circulating BAs are suppressed in DIO mice ($P<0.01$) yet rescued following chronic GcgR agonism (Figure 4a); regulation that is absent in

Gcgr$^{\Delta liver}$ mice (Figure S1h). IUB288 likewise reduced mRNA expression of bile acid regulators *Slc10a1, Cyp27a1, Hmgcr, and Cyp7a1* (Figure 4b)(16) and elevated total and cholic bile acids while decreasing taurodeoxycholic acids in DIO mice (Figure 4c).

Bile acids are ligands of the farnesoid X receptor (FXR/Nr1h4) (15), leading us to investigate FXR signaling in glucagon action. Because both GcgR signaling (5) and FXR (8) are known to regulate *Fgf21* expression, we assessed hepatic *Fgf21* mRNA expression in response to GcgR agonist in WT and FXR-deficient (Fxr$^{-/-}$) mice. Intriguingly, hepatic gene expression and circulating levels of FGF21 were similarly up-regulated in Fxr$^{-/-}$ and in WT control mice (Figure S2a-b, 2-way ANOVA, main effect of treatment, $P<0.01$), suggesting GcgR agonism independently stimulates *Fxr* and *Fgf21* expression.

6-8 w old male WT and FXR$^{-/-}$ mice were treated for 25 d with IUB288 concomitant with HF-feeding to assess the role of FXR in GcgR-mediated prevention of HFD-induced metabolic deffects. GcgR activation prevented HFD-induced BW and fat mass gain in WT but not in FXR-deficient mice (Figure S2c-f), whereas lean mass and food intake remained unaffected in this study (Figure S2g-h). These results indicate that FXR action is a necessary mediator of the GcgR signaling on BW.

Hepatic FXR Mediates GcgR-stimulated Reduction in Obesity.

Since our findings demonstrate that chronic glucagon action reduces BW via the liver, we generated liver-specific *Fxr* knockout mice (*Fxr*$^{\Delta Liver}$) to test the organ-specific contribution of FXR signaling. 6-8 w old WT and *Fxr*$^{\Delta Liver}$ mice exhibited similar BW and

body composition while fed with standard chow (Figure S3a). However, *Fxr*$^{\Delta Liver}$ mice were DIO-resistant compared to WT mice (Figure S3b), despite similar caloric intake (Figure S3c). After the 10-week HF-feeding period, BW-matched mice from each genotype (WT 38.3 ± 1.2 g; *Fxr*$^{\Delta Liver}$ 35.3 ± 1.3 g) received daily injections of vehicle or the GcgR agonist. IUB288-treated WT mice lost 17% of their original BW ($P<0.001$, Figures 4d and S3d), including reductions of fat and lean mass (Figure 4e-f). GcgR agonsim increased intestinal, but not liver, *Gpbar1* mRNA expression in control, but not *Fxr*$^{\Delta Liver}$ mice (Figure S3e). Although GPBAR1/TGR5 signaling induces *Fgf21*(17) and Glp-1(i.e. *Gcg*)(18), neither was differentially regulated in *Fxr*$^{\Delta Liver}$ mice (Table 1 and Figure S1a,b,d). IUB288 efficacy was blunted in *Fxr*$^{\Delta Liver}$ mice, which lost significantly less BW when compared to IUB288-treated WT controls (Figures 4d and S3d). Furthermore, we failed to detect significant changes in either fat or lean mass in IUB288-treated *Fxr*$^{\Delta Liver}$ mice compared to vehicle counterparts (Figure 4e). Notably, WT IUB288-treated mice displayed a small (16%) reduction in food intake over the treatment period that was not observed in FXR$^{\Delta Liver}$ mice (Figure 4f). The anti-obesity effects of GcgR agonism were also associated with reduced epididymal and inguinal adipocyte size, as well as decreased lipid infiltration in BAT (Figure S4).

We assessed plasma samples from these mice to identify systems/pathways that were altered by GcgR agonism in an FXR-dependent manner (Table 1). Plasma GLP-1, insulin, PAI-1, and glucagon levels were not altered by GcgR agonsim. However, IUB288 treatment significantly decreased GIP, Leptin, and TSH levels in WT mice ($P<0.05$), but not *Fxr*$^{\Delta Liver}$ mice. Resistin and ghrelin levels were significantly decreased while T4 (but not T3) levels were significantly increased in both genotypes upon IUB288

treatment. Unlike WT mice, *Fxr*$^{\Delta Liver}$ mice exhibit plasma bile acids accumulation as described(19), and were resistant to IUB288-induced regulation of bile acids (Figure S3f). Together, these data highlight hepatic FXR as a critical mediator of glucagon's anti-obesity action.

Hepatic FXR Mediates GcgR-Stimulated Increases in Energy Expenditure.

To address mechanisms underlying the differential effects GcgR agonism, we conducted indirect calorimetry in IUB288-treated *Fxr*$^{\Delta Liver}$ and WT mice. Food intake was not significantly reduced by this short-term GcgR agonism (Figure S5e-f). Nonetheless, and consistent with our prior reports (5), BW reduction following GcgR agonism in DIO WT mice associated with an increase in light- and dark-phase EE (Figures 5a-b,e and S5a). In contrast, IUB288 had no effect on EE in mice lacking hepatic FXR (Figures 5c-e, and S5b). Likewise, GcgR agonism reduced respiratory quotient (RQ) in WT but not FXR$^{\Delta Liver}$ mice (Figures 5f-g and S5c-d), particularly during the light-phase (Figure 5h). Although EE was elevated in IUB288-treated WT mice, locomotor activity was not augmented by GcgR agonism in either genotype (Figure S5g-h). Altogether, these data suggest that GcgR agonism stimulates EE and fatty acid oxidation (FAOx), and this regulation is dependent upon hepatic FXR.

Hepatic FXR mediates GcgR Regulation of Hepatic Lipid Content and Oxidative Capacity.

Plasma triglycerides trended higher after IUB288 treatment in both WT and *Fxr*$^{\Delta Liver}$ mice (Figure 6a). Conversely, plasma cholesterol was considerably reduced and

plasma β-Hydroxybutyrate was elevated by IUB288 treatment in both genotypes (Figure 6b-c). As in previous studies (Figure 2 and (5)), IUB288-treated WT mice exhibited significantly reduced hepatosteatosis, whereas this effect was blunted in *Fxr*$^{\Delta Liver}$ mice (Figures 6d and S4). Consistent with a greater reduction in hepatic triglyceride content, we also observed increased hepatic *Ppargc1a* expression concomitant with decreased *Ppara*, *Scd1*, and *Srebp1c* expression in WT mice, but not *Fxr*$^{\Delta Liver}$ mice (Figure 6e).

To elucidate potential pathways that may mediate the anti-obesity action of the GcgR-FXR signaling axis we conducted RNA-Sequence analysis on liver samples from IUB288-treated WT and *Fxr*$^{\Delta Liver}$ mice. This uncovered 953 genes differentially regulated by IUB288 treatment in an FXR-dependent manner, as well as 12 genes whose regulation was inverted in *Fxr* deficiency (Figure S6a-b). Top gene ontology enriched pathways included oxidative phosphorylation, Eif2, p70S6K, Sirtuin, and mTOR signaling (Figure 7a). Chip-Sequencing Enrichment Analysis (20) of our dataset identified RXR, LXR, and PPARα as likely upstream regulators (Figure 7b). This analysis uncovered that genes related to bile acid (e.g. *Cyp7b1*, *Fgfr4*, *Nr1h3*) and fatty acid metabolism (e.g. *Nr1h2, Fasn, Apoa4*) were significantly regulated by GcgR activation (Figure 7c). Consistent with a cell autonomous FXR-dependent regulation, IUB288 or glucagon treatment stimulated fatty-acid oxidation in WT primary hepatocytes, but this activation was blunted in hepatocytes from *Fxr*$^{\Delta Liver}$ mice (Figure 6f and S6c). Likewise, liver homogenates from WT mice previously treated with IUB288 displayed enhanced FAOx when compared to vehicle treated controls, whereas this effect is lost in liver homogenates from IUB288-treated *Fxr*$^{\Delta Liver}$ mice (Figure 6g).

Discussion

Glucagon, and by extension GcgR signaling, is a potent regulator of energy balance, glucose and lipid metabolism (1). Attempts to antagonize this critical metabolic pathway and thus reverse hyperglycemia have resulted in unexpected dyslipidemia, questioning whether attenuating or enhancing glucagon action is the appropriate therapeutic approach (21; 22). Thus, an important and emerging question revolves around the identification of downstream mechanisms mediating GcgR action and potential segregation of GcgR-induced hyperglycemia from its anti-obesity actions. In this study, we have investigated the thermogenic and anti-obesity effects of GcgR signaling utilizing IUB288 (5). We identified liver as the tissue of origin for these effects, demonstrating a role for FGF21 as a downstream regulator, and uncovered FXR signaling as an additional pathway that mediates some of the anti-obesity actions of GcgR agonism. We likewise identified increased hepatocyte FAOx as a downstream action stimulated by GcgR agonism in an FXR-dependent manner. We further investigated the contributions of GcgR-mediated regulation of bile acid metabolism, a crucial regulator of whole-body energy balance.

A Hepatic Anti-obesity Signal

Whole body germline disruption (23) or tamoxifen-induced conditional whole-body loss of GcgR(24) function results in protection from DIO upon HFD feeding. Interestingly, our data demonstrate that mice with congenital loss of hepatic *Gcgr* expression were not protected from DIO. Nonetheless, our results demonstrate that IUB288-stimulated BW loss in HFD-fed mice requires intact hepatic *Gcgr* expression. While it is possible that

hypothalamic, GcgR-dependent inhibition of food intake(25), or secondary effects of hepatic factors in other tissues, such as brown and white adipose tissue could be contributing to the weight loss, our observations suggest that GcgR-increased energy expenditure is predominantly due to a hepatic effect.

As with its anti-obesity effects, the beneficial effects of GcgR-signaling on dyslipidemia are well known (1); however, our studies clearly identify hepatic GcgRs as the drivers of reduced plasma cholesterol and liver TGs. It is important to note that lack of hepatic GcgR signaling is sufficient to drive increased hepatic TG accumulation and is consistent with increased dyslipidemia following GcgR antagonism (26). This data highlights both the potential for GcgR agonists as anti-NAFLD therapeutics as well as cautioning against GcgR antagonism.

FGF21 as a Downstream Mediator of GcgRs Anti-obesity Effect.

We previously identified the hepatokine FGF21 as a crucial factor in GcgR-mediated energy metabolism (5). FGF21 null mice fail to respond to GcgR-stimulated prevention of DIO (5). However, in this study high-fat feeding was initiated concurrent with GcgR agonism, and thus, FGF21 was only tested in the context of obesity prevention. In this paradigm, FGF21 was responsible for the entirety of GcgR-mediated energy balance. However, when these studies were moved to an obesity treatment paradigm, a more complex regulatory network emerged. These new studies in an obese model of liver FGF21-deficiency clearly show a blunted body-weight response to chronic GcgR agonism. It is possible that in pre-existing obesity, GcgR agonism stimulates FGF21 secretion from extra-hepatic tissues. However, our findings in $GcgR^{\Delta liver}$ mice support

reports suggesting that the vast majority of circulating FGF21 is hepatically derived (27). Thus, we can surmise that if FGF21 is an important downstream regulator of GcgR action, it must be hepatic in origin. Although FGF21 is a potent anti-obesity signal, it is clear that in the context of GgcR signaling there are both FGF21-dependent and -independent pathways engaged and we must look beyond the FGF21 signaling pathway.

FXR as a parallel GcgR signaling pathway.

Glucagon, via PKA-dependent regulation of HNF4α, modulates hepatocyte *Cyp7a1* expression, the rate-limiting enzyme in bile acid synthesis (28). While this would predictably result in suppression of bile acid synthesis, we also observed suppression of *Slc10a* in IUB288-treated mice. Thus, it is possible that the elevated levels of bile acids observed in circulation are the result, at least in part, of reduced hepatocyte transport at the basolateral membrane(29). Interruption of GcgR signaling (genetic or pharmacological) elevates primary and secondary plasma BAs (9; 26; 30; 31). As compensatory effects of either genetic ablation or pharmacology could underlie these effects, our strategy to combine genetic and pharmacological interventions may provide a more complete view of these GcgR effects. Moreover, fasting which was not controlled for in the cited reports(9; 26; 30; 31), has a profound effect on BA levels.

We observed an elevation in the CA species of bile acids after GcgR agonism. This species is a potent activator of FXR (32) and suggests that glucagon signaling may regulate FXR signaling via BA metabolism. The interplay between BAs and FXR in the regulation of energy expenditure have yet to be fully elucidated. BAs increase energy

expenditure in humans and rodent models of obesity(33-36), but these effects are often attributed to GPBAR1/TGR5, not FXR(37). Of interest, we observed an FXR-dependent increase in intestinal *Gpbar1* expression following GcgR agonsim, providing a line of future focus. Conversely, BA-binding resins reduce serum BAs and are effective to prevent and treat diet-induced obesity(38). Likewise, $FXR^{-/-}$ mice are resistant to diet-induced obesity(39). Consistent with this observation, chronic treatment with a synthetic FXR agonist GW4063 accentuated DIO(40), while FXR inhibition via tauro-β-muricholic acid (T-β-MCA)(41) or glycine-β-muricholic acid (Gly-MCA)(42) correlates with improved metabolic function. Thus, the role of BAs, FXR, and GPBAR1/TGR5 signaling in metabolic regulation warrants continued investigation.

Both GcgR (5) and FXR signaling (8) regulate the expression of FGF21. Here we report similar *Fgf21* expression and circulating FGF21 levels in $Fxr^{-/-}$, $Fxr^{\Delta liver}$, and WT control mice, demonstrating that FXR signaling is dispensible for GcgR-induced FGF21. Therefore, it is plausible that the intermediate effect on body weight observed in both $Fgf21^{\Delta Liver}$ and $Fxr^{\Delta Liver}$ mice, as compared to their appropriate controls, are reciprocal components of the GcgR effect. Although not directly tested here, studies are underway to assess the combined contributions of these two pathways. We also assayed endocrine pathways known to regulate energy balance (i.e. ghrelin, GIP, leptin, resistin, TSH, T3, and T4). However, all of these factors were regulated in a similar manner between WT and $Fxr^{\Delta Liver}$ mice. This suggests that the liver is largely responsible for the FXR-dependent metabolic actions observed during GcgR agonism. Beyond FXR, GcgR activation may increase whole body energy expenditure in part via thyroid hormone. Moreover, increased T4 levels are likely suppressing TSH in these mice. The

suppressed ghrelin observed was a bit unexpected as glucagon administration on isolated rat stomach has been reported to increase ghrelin secretion (43). Whether the observed decrease in ghrelin levels contributes to IUB288-induced BW loss cannot be completely discarded based on our experiments.

Hepatic FXR as a Regulator of Whole-body and Hepatic Energetics.

Glucagon increases oxygen consumption, body temperature, and energy expenditure in rodents (5; 43), and likewise increases energy expenditure and fat oxidation in humans (44; 45). Similarly, FXR regulates energy expenditure (46) and mitochondrial function (47). Our studies suggest that at least a portion of glucagon's anti-obesity action is mediated via hepatic FXR and involves an increase in energy expenditure. Consistent with accumulation of circulating IUB288 (an acylated peptide), EE increased with each subsequent dose and was most evident in final days of indirect calorimetry. DIO *Fxr*$^{\Delta Liver}$ mice were unresponsive to GcgR agonism, even after 5 d of treatment. Moreover, increased EE was independent of changes in locomotor activity, suggesting that GcgR agonism stimulates basal metabolic rate in an FXR-dependent manner. Substrate preference (RQ) was also altered by GcgR agonism. RQ in all mice was suppressed (near 0.74) and indicative of the high-fat feeding. However, GcgR agonism was sufficient to further reduce RQ in WT, but not *Fxr*$^{\Delta Liver}$ mice, suggesting that GcgR signaling stimulates FAOx in an FXR-dependent manner. This, along with the potent reduction in fat mass observed after IUB288 treatment, also suggests that the energetic demands induced by GcgR agonism are met via increased FAOx. Lipolysis may represent one of the main effects of GcgR activation (i.e. to fuel fat utilization). The

amount of free fatty acid released from BAT by glucagon treatment is 10 times higher than that of WAT (48). Therefore, it is plausible that BAT intracellular lipid provides the first source for glucagon-stimulated FAOx, while WAT may represent a later source. Studies are currently underway to address these questions; however, the results described herein confirm prior reports that GcgR agonism stimulates hepatocyte FAOx (49). Regarding the mechanism(s) underlying this elevated oxidative state, we observed an increase in expression of hepatic oxidative phosphorylation genes, and specifically *Ppargc1a*. Of note, overexpression of hepatic PGC-1α is sufficient to increase hepatic mitochondrial respiration and whole-body fat oxidation (50), suggesting that this critical transcriptional co-regulator may also contribute to FAOx and fat mass loss in our system. Likewise, elevated cAMP (as in GcgR signaling) and *Ppargc1a* overexpression both induce *Fxr*(51). Furthermore, PGC-1α interacts with the FXR DNA-binding domain to enhance subsequent FXR-target gene induction (51). Thus, future studies will focus on the interaction of these crucial transcriptional regulators in the context of GcgR signaling.

In conclusion, we report that hepatic Fxr is a critical regulator of glucagon's anti-obesity effects. The metabolic benefits of IUB288 appear to be liver cell autonomous, GcgR-dependent, and mediated through parallel FGF21 and FXR pathways (Figure 7d). These discoveries serve to further highlight the emerging value of fasting-hormone pathways as superior target pathways for the treatment of metabolic disease. Additional dissection of the detailed molecular interactions connecting GcgR activation with FXR

signaling and FGF21 induction may provide novel drug targets for the treatment of metabolic diseases.

Acknowledgments: The project described was supported by the NIH grants 5K01DK098319 and 1R01DK112934 (KMH), and R01 DK077975 (DPT); as well as the UAB Small Animal Phenotyping Core supported by the NIH Nutrition &Obesity Research Center P30DK056336, Diabetes Research Center P30DK079626 and the UAB Nathan Shock Center PAG050886A. This work was also supported by the American Diabetes Association grant 1-13-JF-21 (KMH), CIHR grants 136942 and 154321 and the Canada Research Chairs Program (DJD).

Author Involvement:

TK and KMH were responsible for study conception and design, data analyses and interpretation, and drafting the article; TK, SN, and CS generated experimental data; MP and AW were responsible for RNA-seq analyses; MY, DJD, RD, DP-T, and MHT advised study concept and critical revision of the article. KMH is the guarantor of this work and, as such, had full access to all the data in the study and takes responsibility for the integrity of the data and the accuracy of the data analysis.

Table 1. Hormone profile in plasma samples. N=7 - 10 per group, Mean ± SEM, * P< 0.05, ** P<0.01, **** P< 0.001 within genotype, # P< 0.05 between WT and *Fxr*$^{\Delta Liver}$ in the same treatment.

	WT Vehicle	**WT IUB288**	**FXR$^{\Delta Liver}$ Vehicle**	**FXR$^{\Delta Liver}$ IUB288**
Ghrelin (ng/mL)	30 ± 3.9	15 ± 1.4 *	28 ± 3.4	15 ± 1.7 **
GIP (pg/mL)	384 ± 62	183 ± 18 *	314.7 ± 31.8	264 ± 37
GLP-1 (pg/mL)	38 ± 13	42.1 ± 14	48 ± 17	38 ± 13
PAI-1 (pg/mL)	809 ± 105	493 ± 22.5	856 ± 30.4	739 ± 136
Insulin (ng/mL)	5.4 ± 0.7	4.4 ± 0.5	4.5 ± 0.3	3.8 ± 0.3
Leptin (ng/mL)	12 ± 3	3.6 ± 0.9 *	10.6 ± 1.5	3.0 ± 0.6
Glucagon (pg/mL)	272 ± 27	219 ± 20	303 ± 31	287 ± 19.5
Resistin (ngmL)	109 ± 14	64 ± 8 *	104 ± 6.5	62 ± 8.5 *
TSH (ng/mL)	1.5 ± 0.1	0.8 ± 0.06 *	1.5 ± 0.2	1.0 ± 0.1
T4 (ng/mL)	884 ± 59	1,520 ± 24 ****	607 ± 57 ##	1,320 ± 43 ****,#
T3 (ng/mL)	34 ± 1.8	40 ± 1	23 ± 1.3 ###	33 ± 2.1 *** #

Figure Legends

Figure 1: DIO in *Gcgr*$^{\Delta Liver}$ mice. Total food intake (a) and absolute body weight accrual (b) during 70 d of high-fat (HF) feeding in male, WT and *Gcgr*$^{\Delta Liver}$ mice. Fat and lean (c) mass of mice before (t=0 d) and after (t=70 d) HF-feeding. Glucose tolerance (d) of WT and *Gcgr*$^{\Delta Liver}$ mice following 65d of HF-feeding. All data are represented as mean +/- SEM (n=17-23 mice/group). *P< 0.05, **P< 0.01, ***P< 0.001, **** P< 0.0001, as compared to littermate controls; and #### p< 0.0001 as compared to baseline within genotype.

Figure 2: GcgR agonism in GcgR$^{\Delta Liver}$ mice. Ad libitum blood glucose (a) of DIO WT and *Gcgr*$^{\Delta Liver}$ mice (see Figure 1) following daily GcgR agonism (10 nmol/kg IUB288). Change in (%) body weight (b) and body composition (c) after daily GcgR agonism.

Total food intake (d), plasma (e), and liver (f) triglyceride (TG) and cholesterol (CHL) in DIO WT and *Gcgr*$^{\Delta Liver}$ mice following daily GcgR agonism. All data are represented as mean +/- SEM (n=8-12 mice/group). *P< 0.05, **P< 0.01, ***P< 0.001, ****P< 0.0001, as compared to vehicle controls; and #P< 0.05, ##P< 0.01, ###P< 0.001, ####P< 0.0001 as compared between genotypes within treatment.

Figure 3: GcgR agonism in *Fgf21*$^{\Delta Liver}$ mice. Change in (%) body weight (a) average food intake (b), and body composition (c) of 20 week old male, DIO WT and *Fgf21*$^{\Delta Liver}$ mice following daily GcgR agonism (10 nmol/kg IUB288). All data are represented as mean +/- SEM (n=5-7 mice/group). *P< 0.05, **P< 0.01, ***P< 0.001, ****P< 0.0001, as compared to vehicle controls; and #P< 0.05, ##P< 0.01, ###P< 0.001, ####P< 0.0001 as compared between genotypes within treatment. Mice were maintained on HFD for 12 weeks to induce DIO prior to treatment.

Figure 4: Bile acid regulation and GcgR agonism in *Fxr*$^{\Delta Liver}$ mice. Plasma bile acids (a) in male chow- and HF-fed C57Bl/6J mice following 18d GcgR agonism (10 nmol/kg IUB288). Liver *Slc10a1, Cyp27a1, Hmgcr, and Cyp7a1* mRNA expression (b) in DIO C57Bl/6J mice following 18d GcgR agonism. Plasma bile acid profile (c) in male WT mice following 16d GcgR agonism. Change in (%) body weight (d) day 14 fat and lean mass (e), and food intake (f) of male, DIO WT and *Fxr*$^{\Delta Liver}$ mice following daily GcgR agonism (10 nmol/kg IUB288). All data are represented as mean +/- SEM (n=5-7 mice/group). *P< 0.05, **P< 0.01, ****P< 0.0001, as compared to vehicle controls; and #P< 0.05, ##P< 0.01, ###P< 0.001, ####P< 0.0001 as compared between genotypes/diet within treatment. WT and *Fxr*$^{\Delta Liver}$ mice were placed on HFD at 8-10 weeks old and maintained on HFD for 10 weeks to induce DIO prior to treatment.

Figure 5: Indirect calorimetry during GcgR agonism in *Fxr*$^{\Delta Liver}$ mice. Energy expenditure (EE, kcal/hr) measured during final 72h of 7 d indirect calorimetry analysis (a and c) and average diurnal EE (b and d) in DIO WT (a-b) and *Fxr*$^{\Delta Liver}$ mice (c-d) during daily GcgR agonism (10 nmol/kg IUB288) of WT and *Fxr*$^{\Delta Liver}$ mice (see figure 4). Average EE (final 72h) in vehicle and IUB288 treated mice (e). Respiratory quotient (RQ) during final 72h (f-g) and light phase RQ (h) in DIO WT and *Fxr*$^{\Delta Liver}$ mice during daily GcgR agonism (10 nmol/kg IUB288). IUB288 administered via subcutaneous injection 1hr prior to dark phase (ZT11). All data are represented as mean +/- SEM (n=6 mice/group). *P< 0.05, **P< 0.01, as compared to vehicle controls; and ##P< 0.01, as compared between genotypes within treatment. P-value in (a) and (f) denote main-effect of drug in repeated measures two-way ANOVA.

Figure 6: Liver lipid metabolism and fatty acid oxidation during GcgR agonism in Fxr$^{\Delta Liver}$ mice. Plasma triglyceride (a, TG), cholesterol (b, CHL), and β-Hydroxybutyrate (c) in DIO WT and Fxr$^{\Delta Liver}$ mice following 14 d IUB288 treatment (see Figure 4). Liver TG (d) and change in liver TG (inset), and liver *Ppargc1a, Ppara, Scd1, and Srebp1c* mRNA expression (e) in 14d IUB288-treated DIO WT and *Fxr*$^{\Delta Liver}$ mice. [^{14}C] Palmitate oxidation in primary hepatocytes (f) isolated from WT and *Fxr*$^{\Delta Liver}$ mice and treated with IUB288 for O.N. treatment followed by 3 h incubation with radioactive substrate in serm-free buffer. [^{14}C] Palmitate oxidation in liver tissue homogenates (g) isolated from 6-8 month-old, chow-fed WT and Fxr$^{\Delta Liver}$ mice following 2d IUB288 treatment (n=4-6 mice/group). *P< 0.05, **P< 0.01, ***P< 0.001, ****P< 0.0001, as compared to vehicle controls; and #P< 0.05, ##P< 0.01, ###P< 0.001, ####P< 0.0001 as compared between genotypes within treatment.

Figure 7: Transcriptional Regulation Stimulated by IUB288 Treatment in $Fxr^{\Delta Liver}$ and WT Mice. Gene Set Enrichment Analysis of the 953 Genes differentially expressed only in the IUB288-treated WT vs. Veh-WT was used to generate Top 5 Gene Ontology (GO) Term Enriched Pathways(a). Published ChIP-Sequencing datasets were used to enrich the genes exclusively regulated in wild-type mice (b). FXR-dependent DEGs associated with fatty acid or bile acid metabolism (c). Liver tissues analyzed from mice in Figure 4. Proposed model of mechanisms regulating the anti-obesity effects of glucagon-receptor agonism (d). CA, Cholic Acid; FGF21, Fibroblast Growth Factor 21; FXR, Farnesoid X Receptor; GcgR, Glucagon Receptor.

References

1. Habegger KM, Heppner KM, Geary N, Bartness TJ, DiMarchi R, Tschop MH: The metabolic actions of glucagon revisited. Nat Rev Endocrinol 2010;6:689-697
2. Brown RJ, Sinaii N, Rother KI: Too much glucagon, too little insulin: time course of pancreatic islet dysfunction in new-onset type 1 diabetes. Diabetes Care 2008;31:1403-1404
3. Day JW, Ottaway N, Patterson JT, Gelfanov V, Smiley D, Gidda J, Findeisen H, Bruemmer D, Drucker DJ, Chaudhary N, Holland J, Hembree J, Abplanalp W, Grant E, Ruehl J, Wilson H, Kirchner H, Lockie SH, Hofmann S, Woods SC, Nogueiras R, Pfluger PT, Perez-Tilve D, DiMarchi R, Tschop MH: A new glucagon and GLP-1 co-agonist eliminates obesity in rodents. Nature chemical biology 2009;5:749-757
4. Finan B, Yang B, Ottaway N, Smiley DL, Ma T, Clemmensen C, Chabenne J, Zhang L, Habegger KM, Fischer K, Campbell JE, Sandoval D, Seeley RJ, Bleicher K, Uhles S, Riboulet W, Funk J, Hertel C, Belli S, Sebokova E, Conde-Knape K, Konkar A, Drucker DJ, Gelfanov V, Pfluger PT, Muller TD, Perez-Tilve D, DiMarchi RD, Tschop MH: A rationally designed monomeric peptide triagonist corrects obesity and diabetes in rodents. Nature medicine 2015;21:27-36
5. Habegger KM, Stemmer K, Cheng C, Muller TD, Heppner KM, Ottaway N, Holland J, Hembree JL, Smiley D, Gelfanov V, Krishna R, Arafat AM, Konkar A, Belli S, Kapps M, Woods SC, Hofmann SM, D'Alessio D, Pfluger PT, Perez-Tilve D, Seeley RJ, Konishi M, Itoh N, Kharitonenkov A, Spranger J, DiMarchi RD, Tschop MH: Fibroblast growth factor 21 mediates specific glucagon actions. Diabetes 2013;62:1453-1463
6. Kharitonenkov A, Shiyanova TL, Koester A, Ford AM, Micanovic R, Galbreath EJ, Sandusky GE, Hammond LJ, Moyers JS, Owens RA, Gromada J, Brozinick JT, Hawkins ED, Wroblewski VJ, Li DS, Mehrbod F, Jaskunas SR, Shanafelt AB: FGF-21 as a novel metabolic regulator. J Clin Invest 2005;115:1627-1635
7. Ito S, Fujimori T, Furuya A, Satoh J, Nabeshima Y: Impaired negative feedback suppression of bile acid synthesis in mice lacking betaKlotho. J Clin Invest 2005;115:2202-2208
8. Cyphert HA, Ge X, Kohan AB, Salati LM, Zhang Y, Hillgartner FB: Activation of the farnesoid X receptor induces hepatic expression and secretion of fibroblast growth factor 21. J Biol Chem 2012;287:25123-25138
9. Longuet C, Robledo AM, Dean ED, Dai C, Ali S, McGuinness I, de Chavez V, Vuguin PM, Charron MJ, Powers AC, Drucker DJ: Liver-specific disruption of the murine glucagon receptor produces alpha-cell hyperplasia: evidence for a circulating alpha-cell growth factor. Diabetes 2013;62:1196-1205
10. Sinal CJ, Tohkin M, Miyata M, Ward JM, Lambert G, Gonzalez FJ: Targeted disruption of the nuclear receptor FXR/BAR impairs bile acid and lipid homeostasis. Cell 2000;102:731-744
11. Loyd C, Liu Y, Kim T, Holleman C, Galloway J, Bethea M, Ediger BN, Swain TA, Tang Y, Stoffers DA, Rowe GC, Young M, Steele C, Habegger KM, Hunter CS: LDB1 Regulates Energy Homeostasis During Diet-Induced Obesity. Endocrinology 2017;158:1289-1297

12. Kirchner H, Hofmann SM, Fischer-Rosinsky A, Hembree J, Abplanalp W, Ottaway N, Donelan E, Krishna R, Woods SC, Muller TD, Spranger J, Perez-Tilve D, Pfluger PT, Tschop MH, Habegger KM: Caloric restriction chronically impairs metabolic programming in mice. Diabetes 2012;61:2734-2742
13. Li WC, Ralphs KL, Tosh D: Isolation and culture of adult mouse hepatocytes. Methods Mol Biol 2010;633:185-196
14. Cyphert HA, Alonge KM, Ippagunta SM, Hillgartner FB: Glucagon stimulates hepatic FGF21 secretion through a PKA- and EPAC-dependent posttranscriptional mechanism. PLoS One 2014;9:e94996
15. Chiang JY: Bile acid metabolism and signaling. Compr Physiol 2013;3:1191-1212
16. Chiang JY: Regulation of bile acid synthesis: pathways, nuclear receptors, and mechanisms. J Hepatol 2004;40:539-551
17. Donepudi AC, Boehme S, Li F, Chiang JY: G-protein-coupled bile acid receptor plays a key role in bile acid metabolism and fasting-induced hepatic steatosis in mice. Hepatology 2017;65:813-827
18. Katsuma S, Hirasawa A, Tsujimoto G: Bile acids promote glucagon-like peptide-1 secretion through TGR5 in a murine enteroendocrine cell line STC-1. Biochem Biophys Res Commun 2005;329:386-390
19. Kim I, Ahn SH, Inagaki T, Choi M, Ito S, Guo GL, Kliewer SA, Gonzalez FJ: Differential regulation of bile acid homeostasis by the farnesoid X receptor in liver and intestine. J Lipid Res 2007;48:2664-2672
20. Lachmann A, Xu H, Krishnan J, Berger SI, Mazloom AR, Ma'ayan A: ChEA: transcription factor regulation inferred from integrating genome-wide ChIP-X experiments. Bioinformatics 2010;26:2438-2444
21. Campbell JE, Drucker DJ: Islet alpha cells and glucagon--critical regulators of energy homeostasis. Nature reviews Endocrinology 2015;11:329-338
22. Unger RH, Cherrington AD: Glucagonocentric restructuring of diabetes: a pathophysiologic and therapeutic makeover. The Journal of clinical investigation 2012;122:4-12
23. Conarello SL, Jiang G, Mu J, Li Z, Woods J, Zycband E, Ronan J, Liu F, Roy RS, Zhu L, Charron MJ, Zhang BB: Glucagon receptor knockout mice are resistant to diet-induced obesity and streptozotocin-mediated beta cell loss and hyperglycaemia. Diabetologia 2007;50:142-150
24. Finan B, Clemmensen C, Zhu Z, Stemmer K, Gauthier K, Muller L, De Angelis M, Moreth K, Neff F, Perez-Tilve D, Fischer K, Lutter D, Sanchez-Garrido MA, Liu P, Tuckermann J, Malehmir M, Healy ME, Weber A, Heikenwalder M, Jastroch M, Kleinert M, Jall S, Brandt S, Flamant F, Schramm KW, Biebermann H, Doring Y, Weber C, Habegger KM, Keuper M, Gelfanov V, Liu F, Kohrle J, Rozman J, Fuchs H, Gailus-Durner V, Hrabe de Angelis M, Hofmann SM, Yang B, Tschop MH, DiMarchi R, Muller TD: Chemical Hybridization of Glucagon and Thyroid Hormone Optimizes Therapeutic Impact for Metabolic Disease. Cell 2016;167:843-857 e814
25. Quinones M, Al-Massadi O, Gallego R, Ferno J, Dieguez C, Lopez M, Nogueiras R: Hypothalamic CaMKKbeta mediates glucagon anorectic effect and its diet-induced resistance. Mol Metab 2015;4:961-970
26. Guan HP, Yang X, Lu K, Wang SP, Castro-Perez JM, Previs S, Wright M, Shah V, Herath K, Xie D, Szeto D, Forrest G, Xiao JC, Palyha O, Sun LP, Andryuk PJ, Engel SS,

Xiong Y, Lin S, Kelley DE, Erion MD, Davis HR, Wang L: Glucagon receptor antagonism induces increased cholesterol absorption. J Lipid Res 2015;56:2183-2195
27. Markan KR, Naber MC, Ameka MK, Anderegg MD, Mangelsdorf DJ, Kliewer SA, Mohammadi M, Potthoff MJ: Circulating FGF21 is liver derived and enhances glucose uptake during refeeding and overfeeding. Diabetes 2014;63:4057-4063
28. Song KH, Chiang JY: Glucagon and cAMP inhibit cholesterol 7alpha-hydroxylase (CYP7A1) gene expression in human hepatocytes: discordant regulation of bile acid synthesis and gluconeogenesis. Hepatology 2006;43:117-125
29. Anwer MS, Stieger B: Sodium-dependent bile salt transporters of the SLC10A transporter family: more than solute transporters. Pflugers Arch 2014;466:77-89
30. Yang J, MacDougall ML, McDowell MT, Xi L, Wei R, Zavadoski WJ, Molloy MP, Baker JD, Kuhn M, Cabrera O, Treadway JL: Polyomic profiling reveals significant hepatic metabolic alterations in glucagon-receptor (GCGR) knockout mice: implications on anti-glucagon therapies for diabetes. BMC Genomics 2011;12:281
31. Dean ED, Li M, Prasad N, Wisniewski SN, Von Deylen A, Spaeth J, Maddison L, Botros A, Sedgeman LR, Bozadjieva N, Ilkayeva O, Coldren A, Poffenberger G, Shostak A, Semich MC, Aamodt KI, Phillips N, Yan H, Bernal-Mizrachi E, Corbin JD, Vickers KC, Levy SE, Dai C, Newgard C, Gu W, Stein R, Chen W, Powers AC: Interrupted Glucagon Signaling Reveals Hepatic alpha Cell Axis and Role for L-Glutamine in alpha Cell Proliferation. Cell Metab 2017;25:1362-1373 e1365
32. Sepe V, Festa C, Renga B, Carino A, Cipriani S, Finamore C, Masullo D, Del Gaudio F, Monti MC, Fiorucci S, Zampella A: Insights on FXR selective modulation. Speculation on bile acid chemical space in the discovery of potent and selective agonists. Sci Rep 2016;6:19008
33. Broeders EP, Nascimento EB, Havekes B, Brans B, Roumans KH, Tailleux A, Schaart G, Kouach M, Charton J, Deprez B, Bouvy ND, Mottaghy F, Staels B, van Marken Lichtenbelt WD, Schrauwen P: The Bile Acid Chenodeoxycholic Acid Increases Human Brown Adipose Tissue Activity. Cell Metab 2015;22:418-426
34. Chen X, Yan L, Guo Z, Chen Y, Li M, Huang C, Chen Z, Meng X: Chenodeoxycholic acid attenuates high-fat diet-induced obesity and hyperglycemia via the G protein-coupled bile acid receptor 1 and proliferator-activated receptor gamma pathway. Exp Ther Med 2017;14:5305-5312
35. Teodoro JS, Zouhar P, Flachs P, Bardova K, Janovska P, Gomes AP, Duarte FV, Varela AT, Rolo AP, Palmeira CM, Kopecky J: Enhancement of brown fat thermogenesis using chenodeoxycholic acid in mice. Int J Obes (Lond) 2014;38:1027-1034
36. Zietak M, Kozak LP: Bile acids induce uncoupling protein 1-dependent thermogenesis and stimulate energy expenditure at thermoneutrality in mice. Am J Physiol Endocrinol Metab 2016;310:E346-354
37. Watanabe M, Houten SM, Mataki C, Christoffolete MA, Kim BW, Sato H, Messaddeq N, Harney JW, Ezaki O, Kodama T, Schoonjans K, Bianco AC, Auwerx J: Bile acids induce energy expenditure by promoting intracellular thyroid hormone activation. Nature 2006;439:484-489
38. Kobayashi M, Ikegami H, Fujisawa T, Nojima K, Kawabata Y, Noso S, Babaya N, Itoi-Babaya M, Yamaji K, Hiromine Y, Shibata M, Ogihara T: Prevention and treatment

of obesity, insulin resistance, and diabetes by bile acid-binding resin. Diabetes 2007;56:239-247
39. Prawitt J, Abdelkarim M, Stroeve JH, Popescu I, Duez H, Velagapudi VR, Dumont J, Bouchaert E, van Dijk TH, Lucas A, Dorchies E, Daoudi M, Lestavel S, Gonzalez FJ, Oresic M, Cariou B, Kuipers F, Caron S, Staels B: Farnesoid X receptor deficiency improves glucose homeostasis in mouse models of obesity. Diabetes 2011;60:1861-1871
40. Watanabe M, Horai Y, Houten SM, Morimoto K, Sugizaki T, Arita E, Mataki C, Sato H, Tanigawara Y, Schoonjans K, Itoh H, Auwerx J: Lowering bile acid pool size with a synthetic farnesoid X receptor (FXR) agonist induces obesity and diabetes through reduced energy expenditure. J Biol Chem 2011;286:26913-26920
41. Li F, Jiang C, Krausz KW, Li Y, Albert I, Hao H, Fabre KM, Mitchell JB, Patterson AD, Gonzalez FJ: Microbiome remodelling leads to inhibition of intestinal farnesoid X receptor signalling and decreased obesity. Nat Commun 2013;4:2384
42. Jiang C, Xie C, Lv Y, Li J, Krausz KW, Shi J, Brocker CN, Desai D, Amin SG, Bisson WH, Liu Y, Gavrilova O, Patterson AD, Gonzalez FJ: Intestine-selective farnesoid X receptor inhibition improves obesity-related metabolic dysfunction. Nat Commun 2015;6:10166
43. Kamegai J, Tamura H, Shimizu T, Ishii S, Sugihara H, Oikawa S: Effects of insulin, leptin, and glucagon on ghrelin secretion from isolated perfused rat stomach. Regulatory peptides 2004;119:77-81
44. Salem V, Izzi-Engbeaya C, Coello C, Thomas DB, Chambers ES, Comninos AN, Buckley A, Win Z, Al-Nahhas A, Rabiner EA, Gunn RN, Budge H, Symonds ME, Bloom SR, Tan TM, Dhillo WS: Glucagon increases energy expenditure independently of brown adipose tissue activation in humans. Diabetes, obesity & metabolism 2016;18:72-81
45. Tan TM, Field BC, McCullough KA, Troke RC, Chambers ES, Salem V, Gonzalez Maffe J, Baynes KC, De Silva A, Viardot A, Alsafi A, Frost GS, Ghatei MA, Bloom SR: Coadministration of glucagon-like peptide-1 during glucagon infusion in humans results in increased energy expenditure and amelioration of hyperglycemia. Diabetes 2013;62:1131-1138
46. Zhang Y, Ge X, Heemstra LA, Chen WD, Xu J, Smith JL, Ma H, Kasim N, Edwards PA, Novak CM: Loss of FXR protects against diet-induced obesity and accelerates liver carcinogenesis in ob/ob mice. Mol Endocrinol 2012;26:272-280
47. Lee CG, Kim YW, Kim EH, Meng Z, Huang W, Hwang SJ, Kim SG: Farnesoid X receptor protects hepatocytes from injury by repressing miR-199a-3p, which increases levels of LKB1. Gastroenterology 2012;142:1206-1217 e1207
48. Joel CD: Stimulation of metabolism of rat brown adipose tissue by addition of lipolytic hormones in vitro. The Journal of biological chemistry 1966;241:814-821
49. Longuet C, Sinclair EM, Maida A, Baggio LL, Maziarz M, Charron MJ, Drucker DJ: The glucagon receptor is required for the adaptive metabolic response to fasting. Cell metabolism 2008;8:359-371
50. Morris EM, Jackman MR, Meers GM, Johnson GC, Lopez JL, MacLean PS, Thyfault JP: Reduced hepatic mitochondrial respiration following acute high-fat diet is prevented by PGC-1alpha overexpression. American journal of physiology Gastrointestinal and liver physiology 2013;305:G868-880

51. Zhang Y, Castellani LW, Sinal CJ, Gonzalez FJ, Edwards PA: Peroxisome proliferator-activated receptor-gamma coactivator 1alpha (PGC-1alpha) regulates triglyceride metabolism by activation of the nuclear receptor FXR. Genes Dev 2004;18:157-169

Figure 1

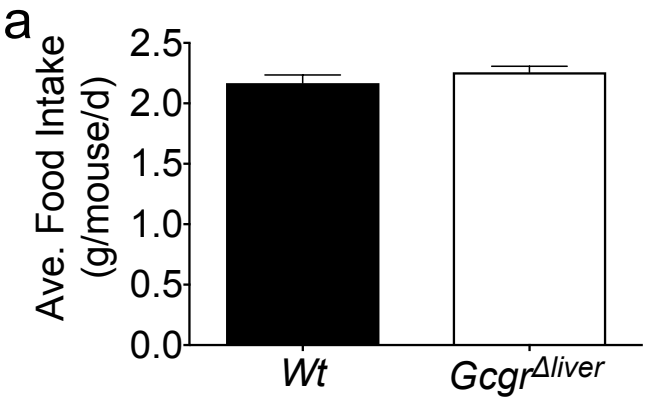
a
Ave. Food Intake (g/mouse/d)
2.5
2.0
1.5
1.0
0.5
0.0
Wt
Gcgr^Δliver

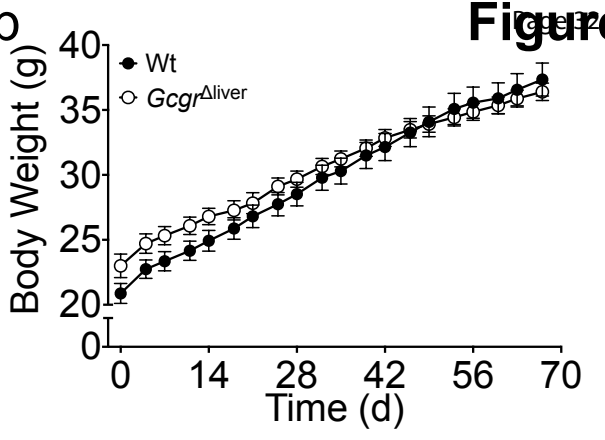
b
Body Weight (g)
40
35
30
25
20
0
Wt
Gcgr^Δliver
0
14
28
42
56
70
Time (d)

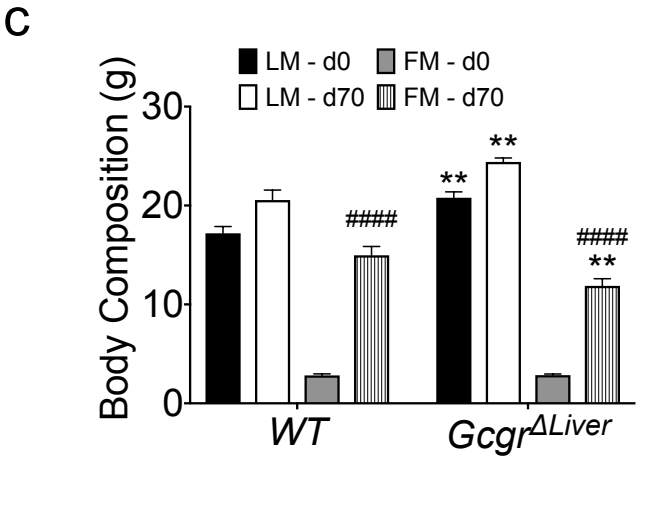
c
Body Composition (g)
LM - d0
FM - d0
LM - d70
FM - d70
30
20
10
0
####
**
**
####
**
WT
Gcgr^ΔLiver

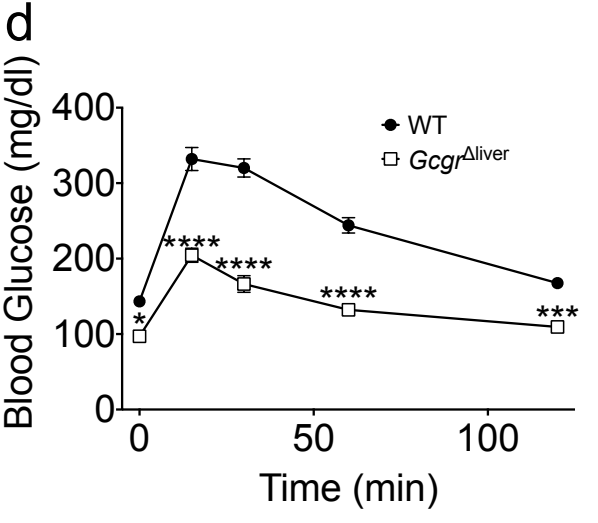
d
Blood Glucose (mg/dl)
400
300
200
100
0
WT
Gcgr^Δliver
*
****
****
****
***
0
50
100
Time (min)

Figure 2

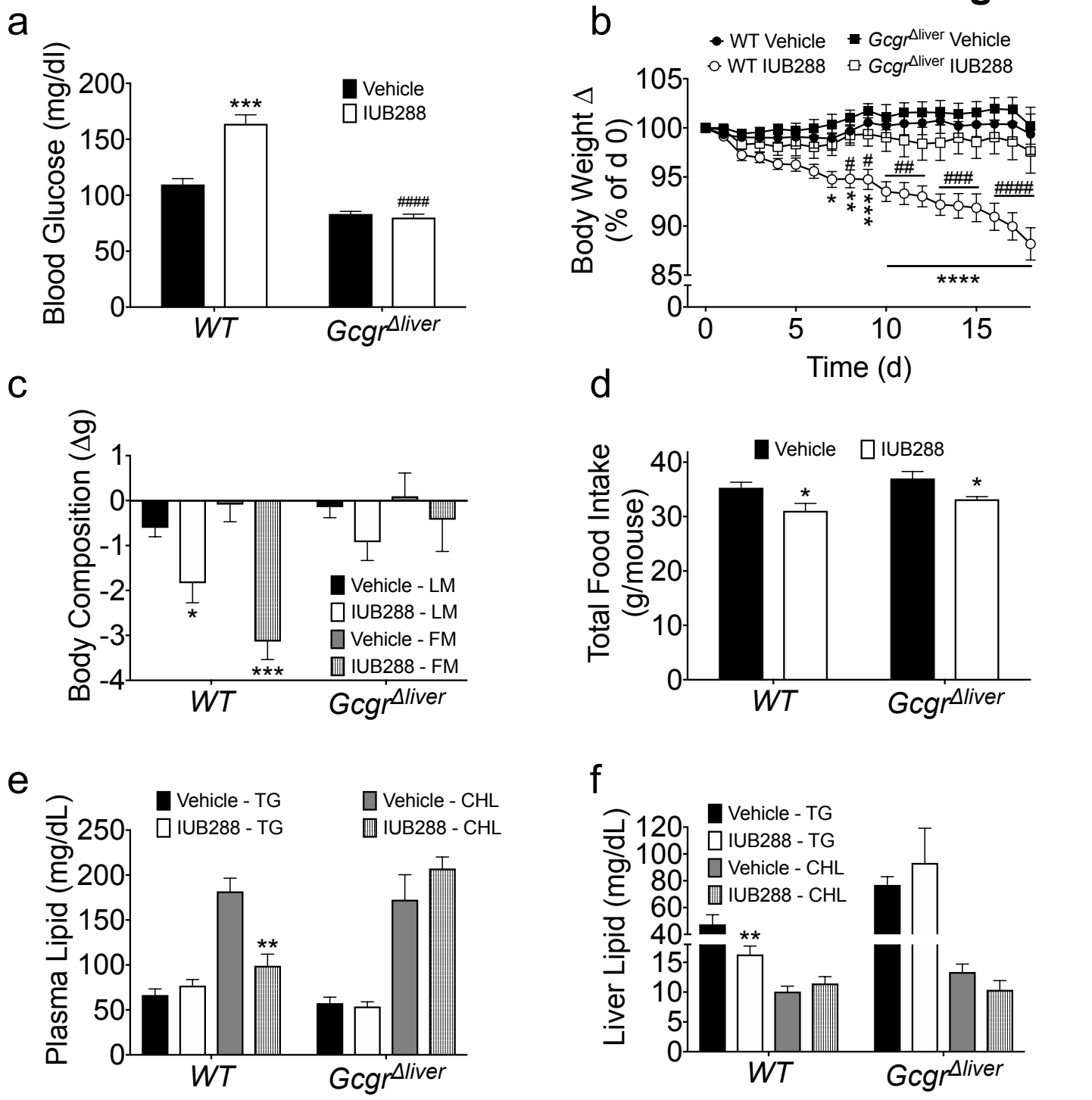
a
Blood Glucose (mg/dl)
200
150
100
50
0
***
Vehicle
IUB288
####
WT
Gcgr^Δliver
b
WT Vehicle
Gcgr^Δliver Vehicle
WT IUB288
Gcgr^Δliver IUB288
Body Weight Δ (% of d 0)
105
100
95
90
85
0
*
***
***
#
#
##
###
####
****
0
5
10
15
Time (d)
c
Body Composition (Δg)
1
0
-1
-2
-3
-4
*
***
Vehicle - LM
IUB288 - LM
Vehicle - FM
IUB288 - FM
WT
Gcgr^Δliver
d
Total Food Intake (g/mouse)
40
30
20
10
0
Vehicle
IUB288
*
*
WT
Gcgr^Δliver
e
Plasma Lipid (mg/dL)
250
200
150
100
50
0
Vehicle - TG
IUB288 - TG
Vehicle - CHL
IUB288 - CHL
**
WT
Gcgr^Δliver
f
Liver Lipid (mg/dL)
120
100
80
60
40
15
10
5
0
Vehicle - TG
IUB288 - TG
Vehicle - CHL
IUB288 - CHL
**
WT
Gcgr^Δliver

Figure 3

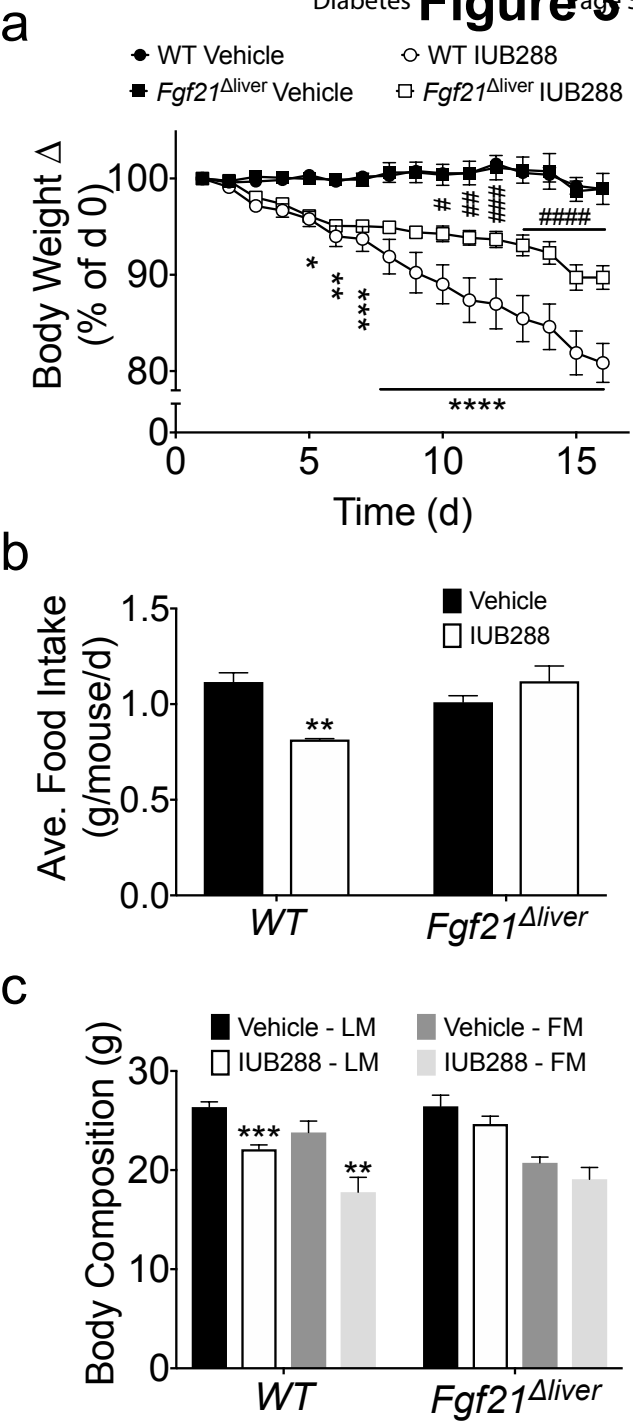
a
WT Vehicle
WT IUB288
Fgf21Δliver Vehicle
Fgf21Δliver IUB288
Body Weight Δ (% of d 0)
100
90
80
0
0
5
10
15
Time (d)
*
**
***
#
##
###
####
****
b
Ave. Food Intake (g/mouse/d)
1.5
1.0
0.5
0.0
Vehicle
IUB288
**
WT
Fgf21Δliver
c
Body Composition (g)
30
20
10
0
Vehicle - LM
IUB288 - LM
Vehicle - FM
IUB288 - FM
***
**
WT
Fgf21Δliver

Figure 4

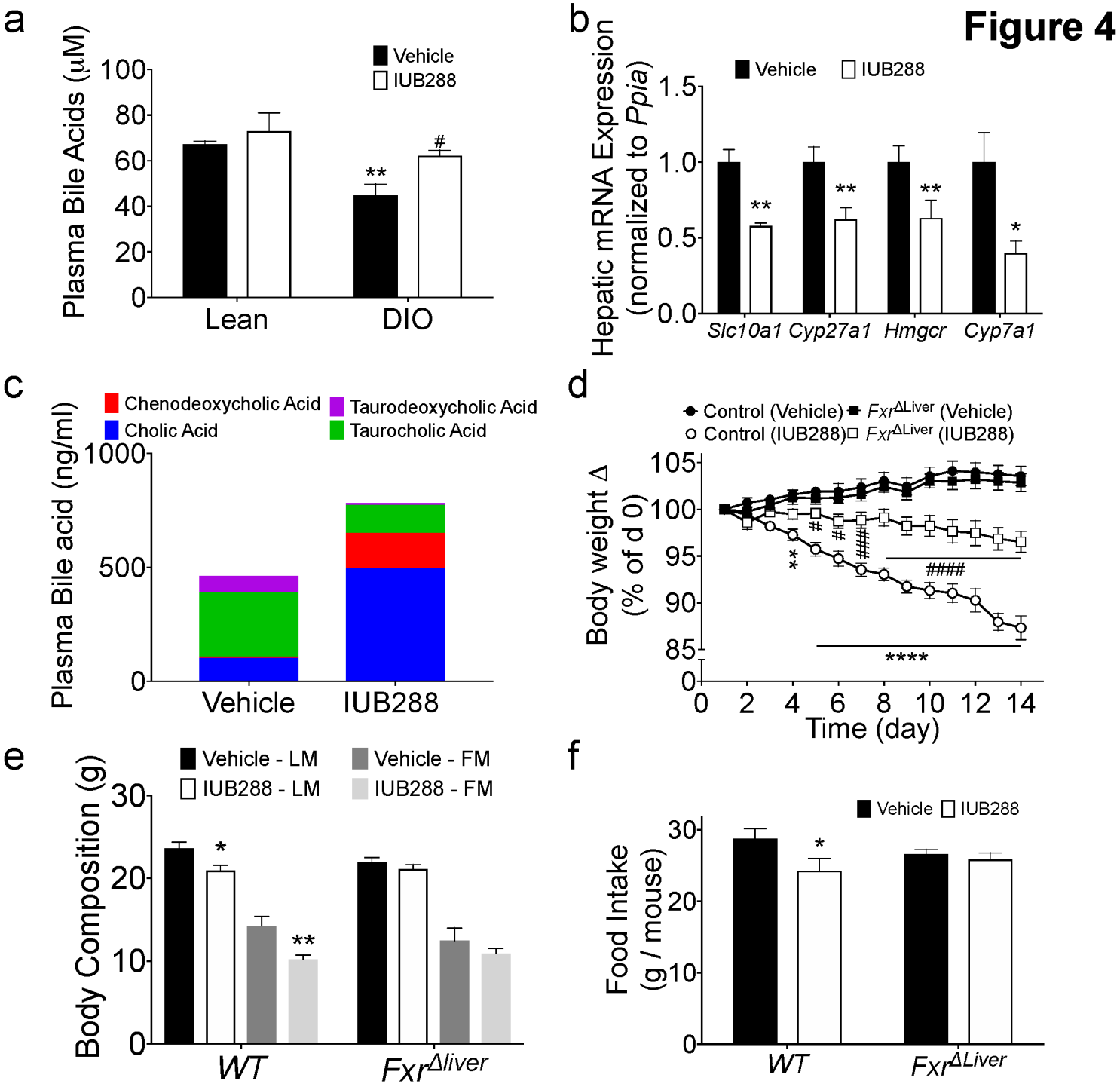
a
Plasma Bile Acids (μM)
Vehicle
IUB288
Lean
DIO
b
Hepatic mRNA Expression (normalized to Ppia)
Vehicle
IUB288
Slc10a1
Cyp27a1
Hmgcr
Cyp7a1
c
Plasma Bile acid (ng/ml)
Chenodeoxycholic Acid
Cholic Acid
Taurodeoxycholic Acid
Taurocholic Acid
Vehicle
IUB288
d
Control (Vehicle)
FxrΔLiver (Vehicle)
Control (IUB288)
FxrΔLiver (IUB288)
Body weight Δ (% of d 0)
Time (day)
e
Vehicle - LM
IUB288 - LM
Vehicle - FM
IUB288 - FM
Body Composition (g)
WT
FxrΔliver
f
Vehicle
IUB288
Food Intake (g / mouse)
WT
FxrΔLiver

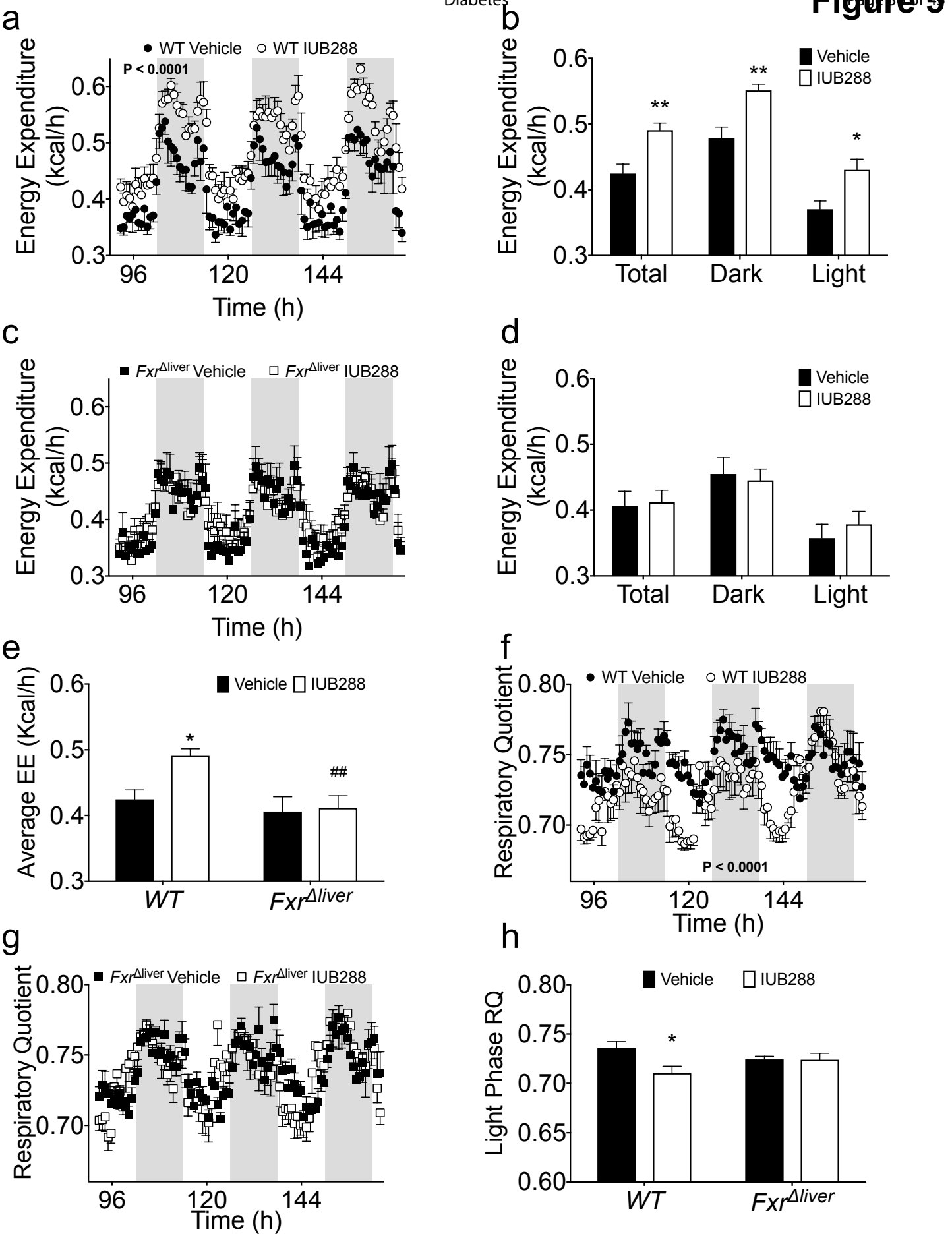
a
WT Vehicle
WT IUB288
P < 0.0001
Energy Expenditure (kcal/h)
Time (h)
b
Vehicle
IUB288
Total
Dark
Light
c
Fxr^Δliver Vehicle
Fxr^Δliver IUB288
d
e
Average EE (Kcal/h)
WT
Fxr^Δliver
f
Respiratory Quotient
g
h
Light Phase RQ

Figure 6

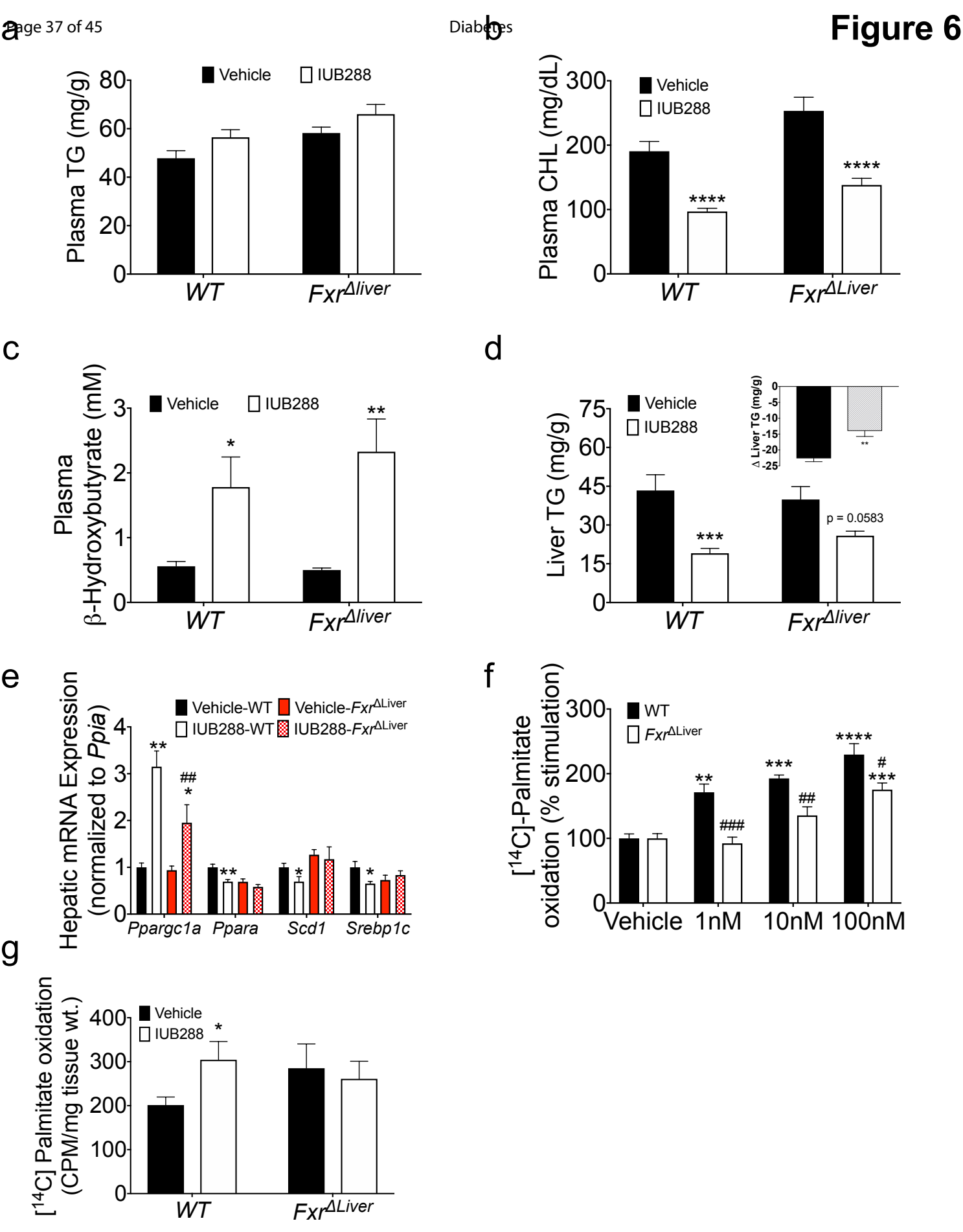
a
Plasma TG (mg/g)
Vehicle
IUB288
WT
Fxr ΔliverΔ
b
Plasma CHL (mg/dL)
Vehicle
IUB288
****
WT
Fxr ΔLiverΔ
c
Plasma β-Hydroxybutyrate (mM)
Vehicle
IUB288
WT
Fxr ΔliverΔ
d
Liver TG (mg/g)
Vehicle
IUB288
Δ Liver TG (mg/g)
p = 0.0583
WT
Fxr ΔliverΔ
e
Hepatic mRNA Expression (normalized to Ppia)
Vehicle-WT
Vehicle-Fxr ΔLiverΔ
IUB288-WT
IUB288-Fxr ΔLiverΔ
Ppargc1a
Ppara
Scd1
Srebp1c
f
[14C]-Palmitate oxidation (% stimulation)
WT
Fxr ΔLiverΔ
Vehicle
1nM
10nM
100nM
g
[14C] Palmitate oxidation (CPM/mg tissue wt.)
Vehicle
IUB288
WT
Fxr ΔLiverΔ

Figure 7

a

GO Term Enriched Pathways

Ingenuity Canonical Pathways	-Log (p-value)	Pathway Enrichment
Eif2 Signaling	29.6	28.5%
Regulation of p70S6K Signaling	8.28	17.8%
Oxidative Phosphorylation	7.65	20.2%
Sirtuin Signaling Pathway	7.55	13.4%
mTOR Signaling	6.46	14.4%

b

Transcriptional Regulation

Transcription Factor	Overlap	P-value	FDR	PMID
LXR	192/2000	1.0E-21	6.5E-19	22158963
RXR	185/2000	4.0E-19	1.3E-16	22158963
PPARa	177/2000	2.3E-16	5.0E-14	22158963
C/EBPa	53/589	8.4E-06	2.2E-04	23403033
FOXO1	32/347	3.2E-04	5.3E-03	23066095
ESR1	38/444	4.2E-04	6.4E-03	17901129
PXR	67/939	7.4E-04	9.5E-03	20693526

c

Top Enriched Gene Association Network: Lipid Metabolism

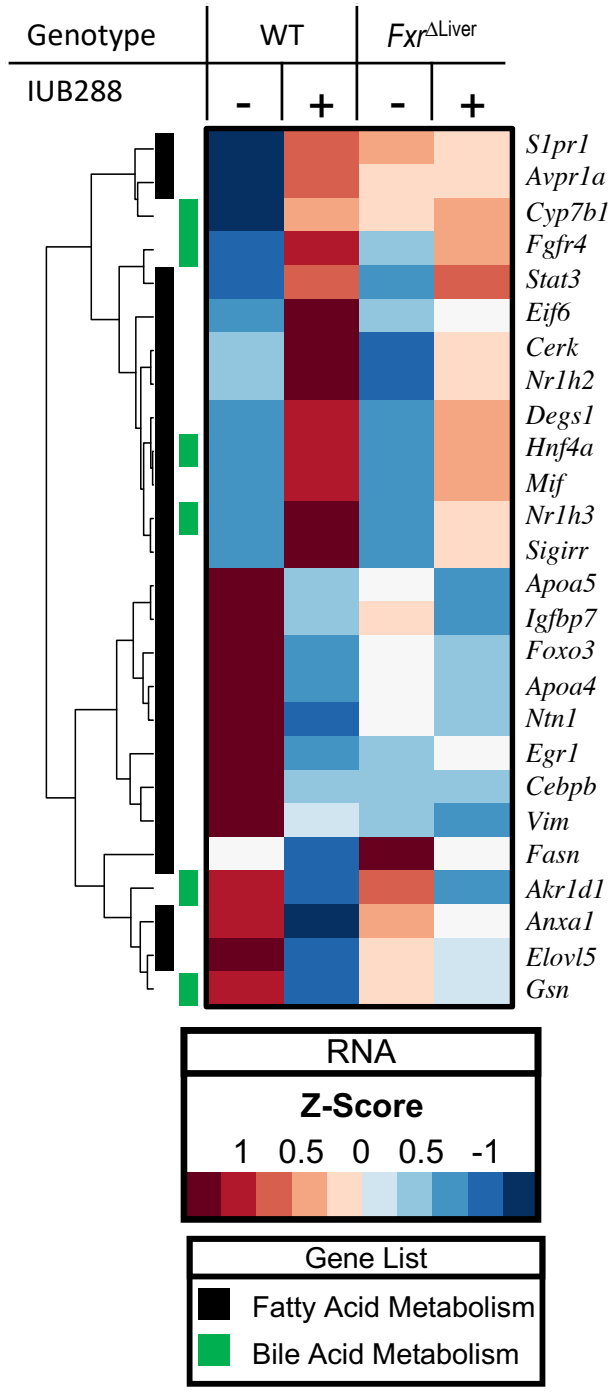

d

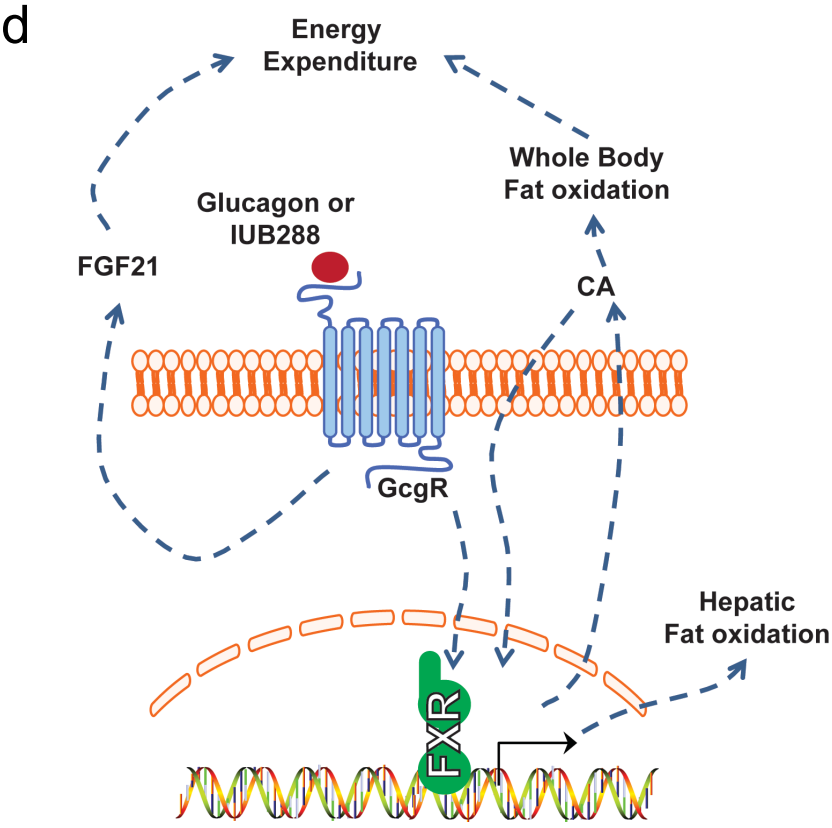

Supplemental Figure 1

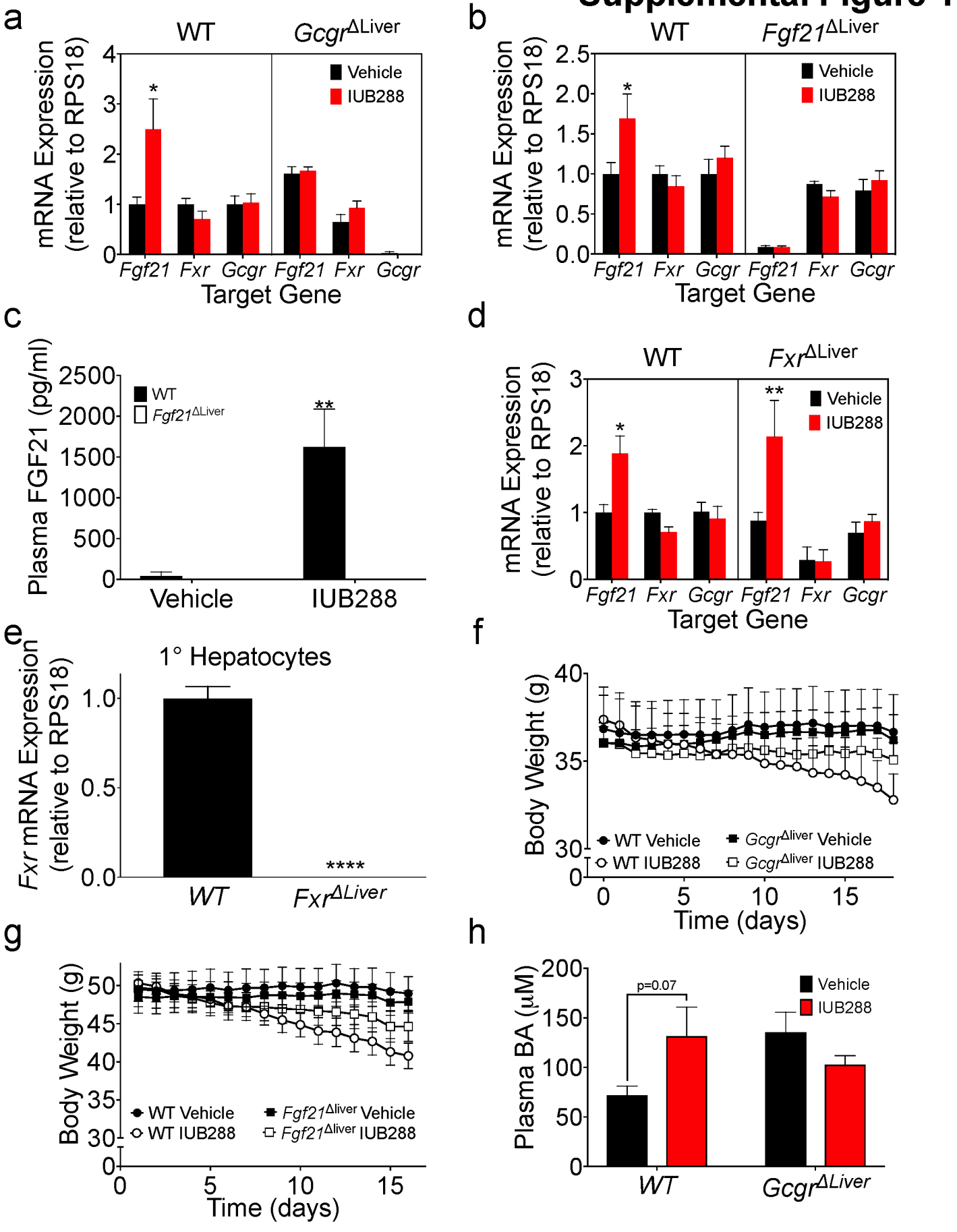

Supplemental Figure 2

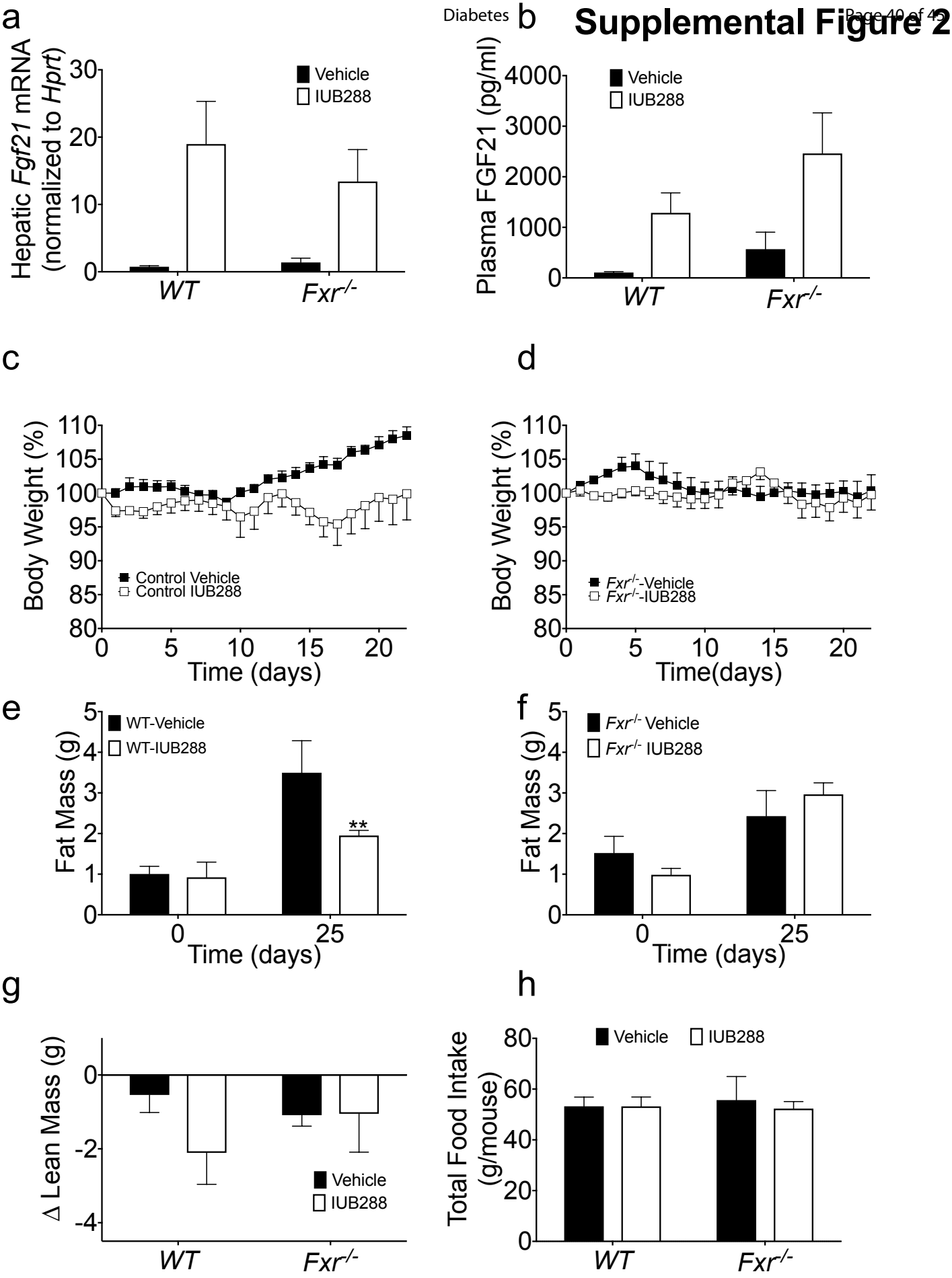

Supplemental Figure 3

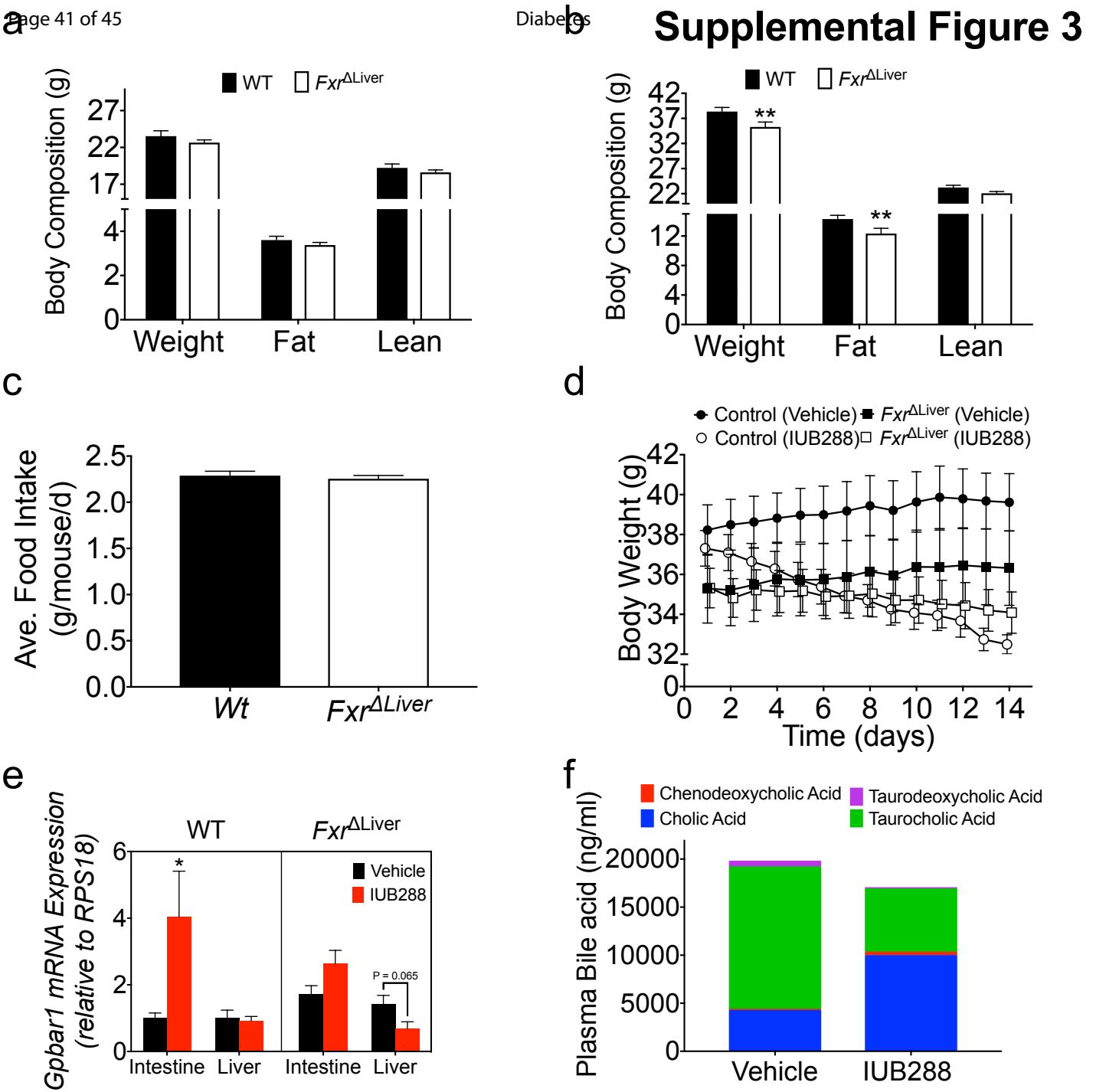

Supplemental Figure 4

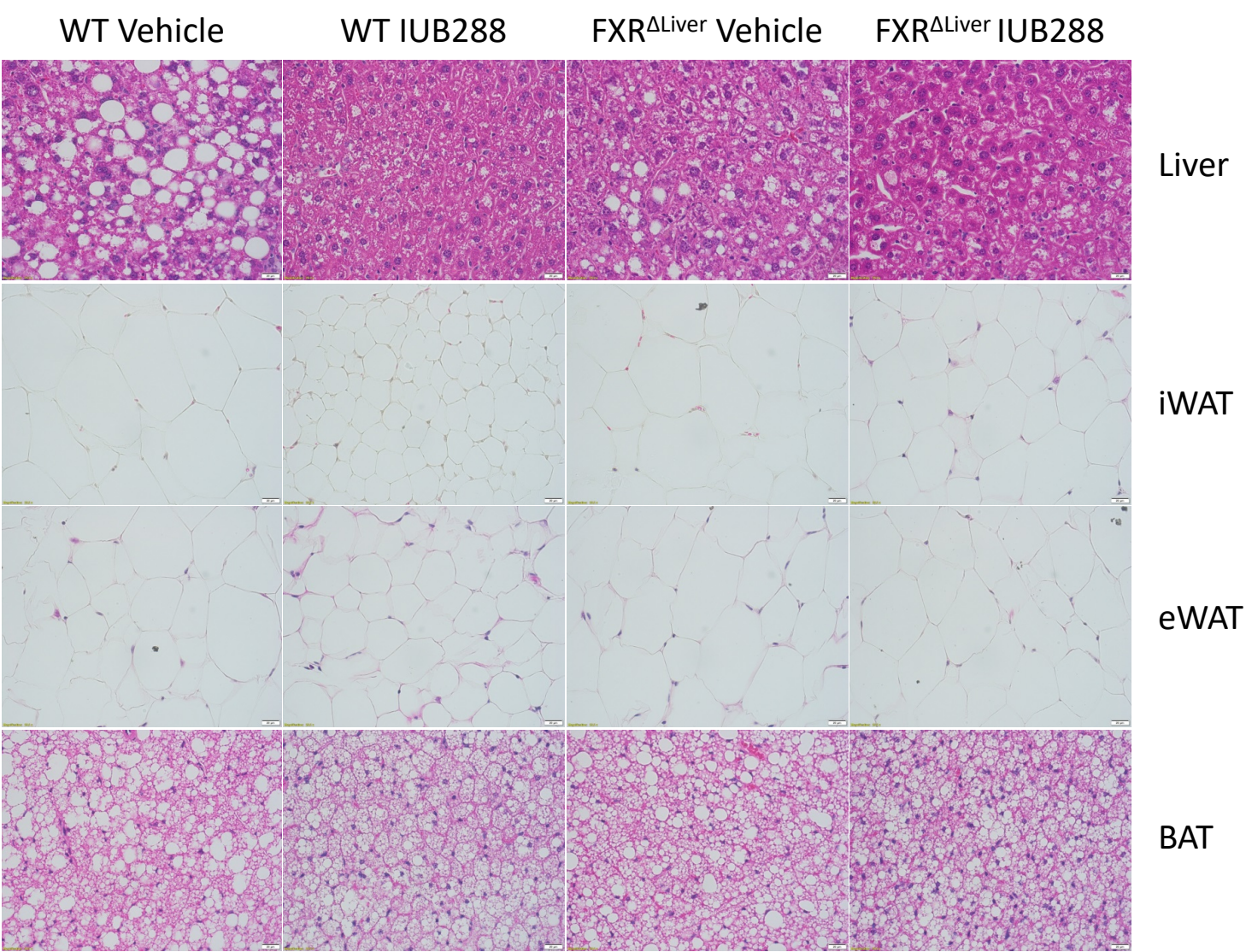

Supplemental Figure 5

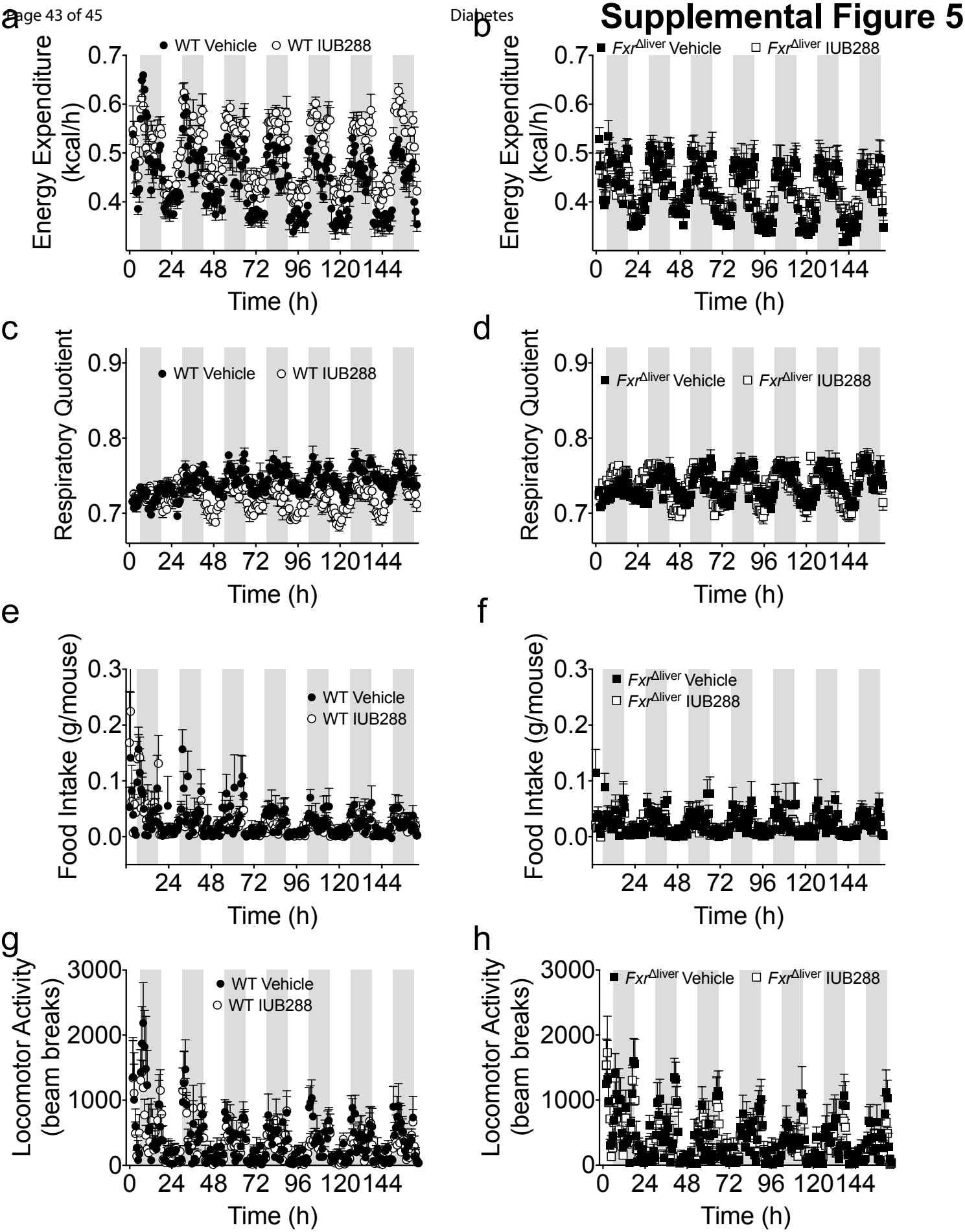

Supplemental Figure 6

a

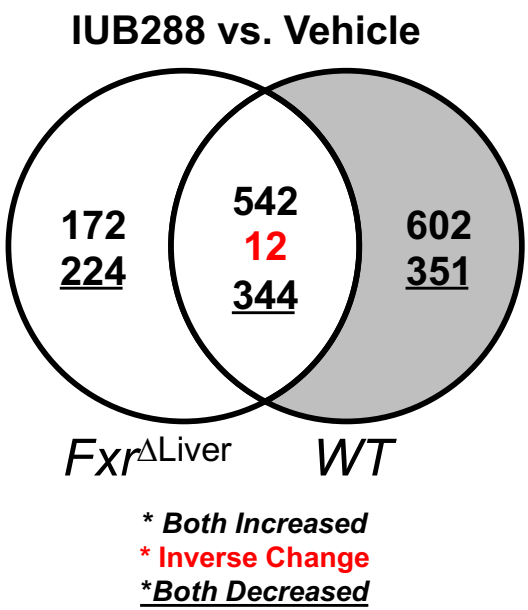

b

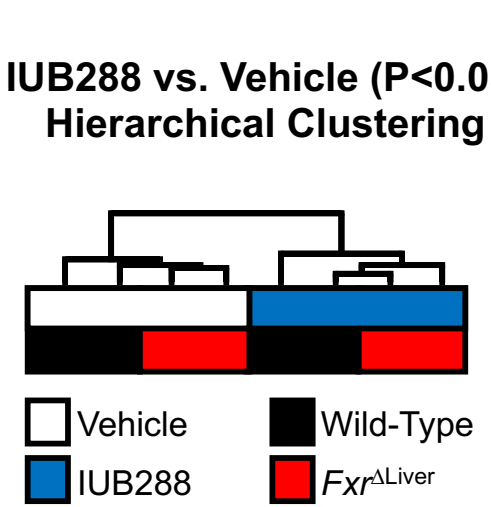

c

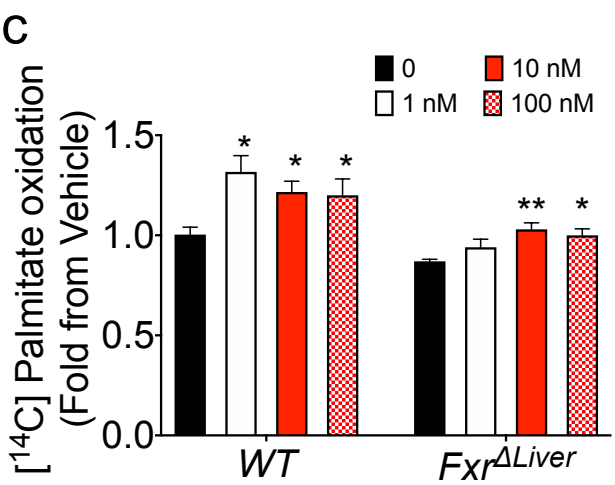

Supplemental Figure Legends:

Figure S1: Model validation and GcgR agonism in GcgR$^{\Delta Liver}$ and Fgf21$^{\Delta Liver}$ mice. mRNA expression of *Gcgr*, *Fgf21*, and *Fxr* in GcgR$^{\Delta Liver}$, Fgf21$^{\Delta Liver}$, Fxr$^{\Delta Liver}$, and littermate Control mice (a, b, and d, n=6-10 mice/group, see Figures 2-4). Plasma FGF21 in 8-week-old, chow fed Fgf21$^{\Delta Liver}$ and littermate Control (WT) mice following 5d Vehicle or IUB288 treatment (c, 10 nmol/kg IUB288, n=4-10 mice/group). *Fxr* mRNA expression in primary hepatocytes isolated from 8-10 week old, chow fed Fxr$^{\Delta Liver}$ or littermate control (WT) mice (e). Body weight of DIO WT and GcgR$^{\Delta Liver}$ mice (f, n=8-12 mice/group) or WT and Fgf21$^{\Delta Liver}$ mice (g, n=5-7 mice/group) following daily GcgR agonism (10 nmol/kg IUB288). Plasma bile acid levels in IUB288-treated DIO WT and GcgR$^{\Delta Liver}$ mice after 2 h fast (h, n=8-12 mice/group, see Figure 2). All data are represented as mean +/- SEM.

Figure S2: GcgR agonism and energy balance in FXR$^{-/-}$ mice. Hepatic *Fgf21* mRNA expression (a) and plasma levels (b) in HF-fed WT and FXR$^{-/-}$ mice. Body weight (%) and fat mass of HF-fed WT (c and e) or FXR$^{-/-}$ mice (d and f) following daily GcgR agonism (10 nmol/kg IUB288). Change in lean mass (g) and total food intake (h) in HF-fed WT or FXR$^{-/-}$ mice. All data are represented as mean +/- SEM (n=3-8 mice/group). **p< 0.01. Male, WT and Fxr$^{-/-}$ mice were placed on HFD at 8-10 weeks old concurrent with IUB288 treatment.

Figure S3: DIO and GcgR agonism in FXR$^{\Delta Liver}$ mice. Body composition before (a) and after (b) HF-feeding in WT and FXR$^{\Delta Liver}$ mice (n=13-15 mice/group). Average food intake (c) during HF-fat feeding in WT and FXR$^{\Delta Liver}$ mice (n=13-15 mice/group). Body weight (d) during daily GcgR agonism (10 nmol/kg IUB288) in WT and FXR$^{\Delta Liver}$ mice (n=8-10 mice/group). Intestine and liver *Gpbar1*/*Tgr5* mRNA expression (e) in 14d IUB288-treated DIO WT and Fxr$^{\Delta Liver}$ mice. Plasma bile acid profile (f) in male Fxr$^{\Delta Liver}$ mice following 16d GcgR agonism. *p< 0.05, **p< 0.01. Male, WT and Fxr$^{\Delta Liver}$ mice were placed on HFD at 8-10 weeks old and maintained on HFD for 10 weeks to induce DIO prior to treatment.

Figure S4: Liver and Adipose Tissue morphology following GcgR agonism in FXR$^{\Delta Liver}$ mice. Representative haemotoxylin and eosin (H & E) staining of liver, inguinal white adipose tissue, ependymal white adipose tissue, and interscapular brown adipose tissue following 14d IUB288 treatment. Male, WT and Fxr$^{\Delta Liver}$ mice were placed on HFD at 8-10 weeks old and maintained on HFD for 10 weeks to induce DIO prior to treatment. Scale bars are 20 μm in length.

Figure S5: 7 d indirect calorimetry during GcgR agonism in Fxr$^{\Delta Liver}$ mice. Energy expenditure (EE, a-b), respiratory quotient (RQ, c-d), food intake (e-f), and locomotor activity (g-h) measured during 7 d indirect calorimetry analysis (in DIO WT (a,c,e, and g) and Fxr$^{\Delta Liver}$ mice (b,d,f, and h) during daily GcgR agonism (10 nmol/kg IUB288). IUB288 administered via subcutaneous injection 1hr prior to dark phase (ZT11). All data are represented as mean +/- SEM (n=6 mice/group, see Figure 5).

Figure S6: Transcriptional Analysis of IUB288 Treatment in Fxr$^{\Delta Liver}$ and WT Mice. (a) Venn diagram illustrating the selection of FXR-dependent DEGs (shaded). (b) Hierarchical clustering of IUB288 vs. Vehicle comparison ($p < 0.05$). (c) [^{14}C] Palmitate oxidation in primary hepatocytes isolated from DIO WT and

$Fxr^{\Delta Liver}$ mice and treated with glucagon for O.N. treatment followed by 3 hr incubation with radioactive substrate.

Supplemental Table 1: qPCR primers

Gene	**Forward (5'-3')**	**Reverse (5'-3')**
Gcgr	GCCAGCGAGGTCTCCATA	ACATCATTCACCTTCTTGTGG
Fgf21	CTG CTG GGG GTC TAC CAA G	CTG CGC CTA CCA CTG TTC C
Scl10a1	GCCACACTATGTACCCTACGTCCTC	GAATGTAGCCCATCAGGAAGCCAGTG
Cyp27a1	GAAGGACCACCGAGACCACAAGG	CGT TTA AGG CAT CCG TGT AGA GCG
Hmgcr	GTGTTCAAGGAGCATGCAAAG	AGCCATCACAGTGCCACATAC
Cyp7a1	GGGATTGCTGTGGTAGTGAGC	GGTATGGAATCAACCCGTTGTC
Fxr	CACAGCGATCGTCATCCTCTCT	TCTCAGGCTGGTACATCTTGCA
Gpbar1/Tgr5	AAGAGCCAAGAGGGACAATC	GTAGCTGCTGCTTCCCTAAT
Ppargc1a	CCCTGCCATTGTTAAGACC	TGCTGCTGTTCCTGTTTTC
Ppara	AGCAGTGCTGGCTACCTTCAA	AATATGTAGCCACCCCCTTGG
Scd1	TCAGAAACACATGCTGATCCTCAT	TGGGTGTTTGCGCACAAG
Srebp1c	GAGGACCTTTGTCATTGGCTG	TACAGAGCAAGAGGGTGCCAT
Hprt	AAGGAGATGGGAGGCCAT	GTTGAGAGATCATCTCCACCAAT
Rps18	TTCTGGCCAACGGTCTAGACAAC	CCAGTGGTCTTGGTGTGCTGA
Ppia	CAGACGCCACTGTCGCTT T	TGTCTTTGGAACTTTGTCTG